Agenzia nazionale per le nuove tecnologie,
l'energia e lo sviluppo economico sostenibile

MINISTERO DELLO SVILUPPO ECONOMICO

Circe experimental report

M. Tarantino, P. Gaggini, I. Di Piazza P. Agostini, N. Forgione,
D. Martelli, G. Barone

Report RdS/2013/046

CIRCE EXPERIMENTAL REPORT

M. Tarantino, P. Gaggini, I. Di Piazza, P. Agostini (ENEA), N. Forgione, D. Martelli, G. Barone (UNIPI)

Settembre 2013

Report Ricerca di Sistema Elettrico

Accordo di Programma Ministero dello Sviluppo Economico - ENEA
Piano Annuale di Realizzazione 2012
Area: Produzione di energia elettrica e protezione dell'ambiente
Progetto: Sviluppo competenze scientifiche nel campo della sicurezza nucleare e collaborazione ai programmi internazionali per il nucleare di IV Generazione
Obiettivo: Sviluppo competenze scientifiche nel campo della sicurezza nucleare
Responsabile del Progetto: Mariano Tarantino, ENEA

Titolo

CIRCE EXPERIMENTAL REPORT

Descrittori

Tipologia del documento: Rapporto Tecnico

Collocazione contrattuale: Accordo di programma ENEA-MSE su sicurezza nucleare e reattori di IV generazione

Argomenti trattati: Termoidraulica
Tecnologia dei Metalli Liquidi
Generation IV Reactors

Sommario

Since the Lead-cooled Fast Reactor (LFR) has been conceptualized in the frame of GEN IV International Forum (GIF), ENEA is strongly involved on the HLM technology development. Currently ENEA has implemented large competencies and capabilities in the field of HLM thermal-hydraulic, coolant technology, material for high temperature applications, corrosion and material protection, heat transfer and removal, component development and testing, remote maintenance, procedure definition and coolant handling.In this frame the CIRCE pool facility has been refurbished to host a suitable test section able to thermal-hydraulically simulate the primary system of a HLM cooled pool reactor.In particular a fuel pin bundle simulator (FPS) has been installed in the CIRCE pool. It has been conceived with a thermal power of about 1 MW and a linear power up to 25 kW/m, relevant values for a LMFR. It consist of 37 fuel pins (electrically simulated) placed on a hexagonal lattice.The LBE, heated by the FPS, flows up through the riser, reaching the Heat Exchanger (HX) inlet though a gas separator placed in the tank upper zone. The primary fluid circulation occurs employing a gas lift system which injects Argon from a nozzle connected to the riser entrance, enhancing the LBE flow. The heat exchanger represents the heat sink of the system and it is designed to have a thermal duty of about 800 kW; it consists of 91 double-wall bayonet tubes (with helium gap) fed by low pressure boiling water. Finally the decay heat removal system (DHR), designed to remove 40 kW and uncoupled from the main flow path. It consists of a bayonet element in which the air is injected from the top, flows downward through the inner tube and then flows upward through the annular region, where heat is removed from primary LBE side. The bayonet element is placed into a suitable shell thermally insulated from the external pool. LBE enters into the shell from the top and flows downwards in a counter flow heat exchanger configuration. The experimental campaign was designed to study the PLOHS+LOF accident, with decay heat removed by the DHR-system. This paper reports the experimental data as well as a preliminary analysis and discussion of the results, focusing on the most relevant tests of the campaign, namely Test IV Temperatures along the three sections of the FPS were reported and the Nusselt number in the FPS sub-channels was investigated . Moreover, the void fraction in the riser was computed and the riser inlet and outlet average temperatures were discussed. Concerning the HX, temperature measurements in the sub-channels were presented, as well as temperatures at the inlet and outlet sections. For the DHR-system, temperatures at the entrance and exit section were analyzed both for the primary lead bismuth eutectic (LBE) circuit and for the secondary air side, estimating the thermal power removed by DHR under the formulated accidental scenario. Finally system codes thermal hydraulics analyses performed adopting the RELAP5/Mod3.3 are presented. A comparison with the data obtained from preliminary experimental tests is presented.

Note

Autori: M. Tarantino, P. Gaggini, I. Di Piazza, P. Agostini (ENEA)
N. Forgione, D. Martelli, G. Barone (UNIPI)

Copia n. **In carico a:**

REV.	DESCRIZIONE	DATA		REDAZIONE	CONVALIDA	APPROVAZIONE
2			NOME			
			FIRMA			
1			NOME			
			FIRMA			
0	EMISSIONE	18/09/2013	NOME	M. Tarantino	A. Del Nevo	M. Tarantino
			FIRMA			

Index

1. THE CIRCE FACILITY AND ICE TEST SECTION

The main objective of CIRCE-ICE experiment is the characterization of mixed convection and stratification phenomena in a heavy liquid metal pool in a safety relevant situation, i.e. during the transition from nominal flow to natural circulation (Loss Of Flow Accident, LOFA) typical of Decay Heat Removal (DHR) conditions. In addition, the Fuel Pin Simulator (FPS), an electrical pin bundle, is instrumented in order to characterize the convective heat transfer in different sub-channels of a HLM-cooled Fuel Assembly.

CIRCE basically consists of a cylindrical vessel (Main Vessel S100) filled with about 70 tons of molten Lead-Bismuth Eutectic (LBE) with argon cover gas and recirculation system, LBE heating and cooling systems, several test sections welded to and hung from bolted vessel heads for separate-effects and integral testing, and auxiliary equipment for eutectic circulation [1-4]. The facility is completed by a LBE storage tank (S200), a small LBE transfer tank (S300) and the data acquisition system (see Figure 1).

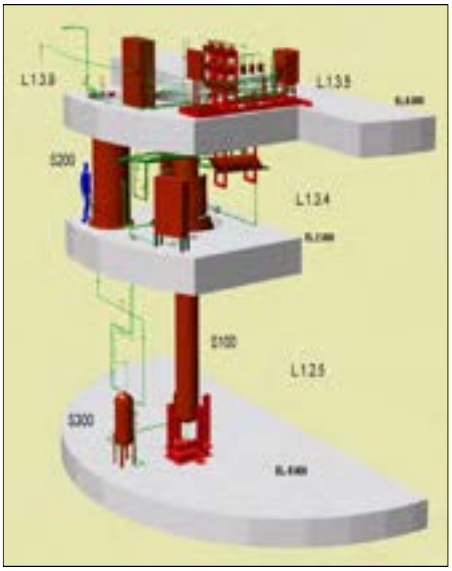

Figure 1 CIRCE isometric view.

During the loading operations, the LBE is gradually transferred from the storage tank (S200) to the S300 vessel. Then, by pressurization of the S300 cover gas, the liquid metal gradually fills the test vessel (S100) from the bottom.

The main vessel S100 consists of a vertical vessel 8500 mm height, connected by gates to the other vessels. It is externally equipped with electrical heating cables, installed at the bottom and on the lateral surface. This heating system operates in a temperature range of 200-400°C.

A skimming line and a passive pressure safety system are also present in the main vessel, in order to guarantee the LBE top level and to prevent accidental overpressure. The S100 parameters are summarized in Table 1.

Table 1: CIRCE S100 main parameters

Parameter	*Value*
Outside Diameter	1200 mm
Wall Thickness	15 mm
Material	AISI 316L
Max LBE Inventory	90000 kg
Electrical Heating	47 kW
Cooling Air Flow Rate	3 Nm^3/s
Temperature Range	200-550°C
Operating Pressure	15 kPa (gauge)
Design Pressure	450 kPa (gauge)
Nominal Argon Flow Rate	15 Nl/s
Argon Injection Pressure	600 kPa (gauge)

The ICE test section is contained in the S100 main vessel and it is designed to reproduce thermal-hydraulic behavior of the XT-ADS and EFIT primary system [5-9]. In Table 2 the experimental parameters characterizing the ICE activity are reported and compared with the foreseen XT-ADS and EFIT concepts ones.

Schematic views of ICE test section, placed in the CIRCE main vessel (S100), are reported in Figure 2.

As can be seen in Figure 2, the ICE test section consists of the following main components:

- *Downcomer*: is the volume between the test section and the main vessel, which allows the hydrodynamic connection between the outlet section of the HX and the inlet section of the feeding conduit.
- *Flow Meter*: is a Venturi-nozzle flow meter. Bubble tubes are adopted to measure the pressure difference through the throat of the nozzle. The flow meter is directly connected to the HS, without a bypass, thus measuring the primary flow rate through the pin bundle.
- *Fuel Pin Simulator* (FPS): is a mechanical structure needed to take on the Heat Source (HS). It is connected in the lower section to the flow meter and in the upper section to the insulation volume by means of the coupling flange. The coupling flange assures the sealing, avoiding the insulation volume flooding by LBE. In the upper section, the FPS is hydraulically linked to the fitting volume, ensuring continuity of the main flow path.
- *Fitting Volume*: is placed in the middle part of the test section, allowing the hydraulic connection between the HS and the riser.
- *Riser*: is an insulated pipe (double wall pipe with air in the gap) connecting the fitting volume with the separator. A nozzle is installed in the lower section to allow the argon injection inside this pipe [10-11].

Table 2: ICE parameters compared with the XT-ADS and EFIT ones.

Parameter	***XT-ADS***	***EFIT***	***ICE***
Coolant	LBE	Pure Lead	LBE
Primary Loop Circulation	Mechanical Pump	Mechanical Pump	Gas Lift Technique
Fuel Assembly Lattice	Hexagonal	Hexagonal	Hexagonal
Fuel Assembly Type	Wrapper	Wrapper	Wrapper
Fuel Assembly Spacer	Grid	Grid	Grid
Fuel Pin Diameter (d) [mm]	6.55	8.72	8.2
Pitch to Diameter Ratio (p/d)	1.41	1.56	1.8
Fuel Heat Flux q'' [MW/m^2]	0.85-1.15	1-1.40	1.00
Fuel Power Density q''' [W/cm^3]	500-700	450-650	488
Average Velocity Fuel Pin Region w_0 [m/s]	1	1	1
Fuel Pin Active Length L [mm]	600	900	1000
T_{inlet}/T_{outlet} core [°C]	300/400	400/480	300/400
$\Delta T_{HS}/L$ [°C/m]	167	88	100
Fuel Pin Clad Material	T91	T91	AISI 316L
Secondary Coolant	Low Pressure Boiling Water	Water with superheated steam	Low pressure boiling Water

- *Separator*: is a volume needed to connect the riser with the HX. It allows the separation of the LBE flowing downward into the HX from the Argon flowing in the test section cover gas through the free surface. Moreover, the separator assures that the overall LBE flow rate flows directly into the HX (shell – side) before falling down in the downcomer. In addition, the separator works as an expansion vessel, allowing for fluid expansion during transient operations.
- *Heat Exchanger:* corresponds to the heat sink of the system. It consists of double-wall bayonet tubes (with helium gap) fed by low pressure boiling water. It has a thermal duty of 800 kW. In order to promote natural circulation along the primary flow path, it is installed in the upper part of the test section.
- *Dead Volume*: is a component made of two concentric pipes. The inner pipe is connected, by bolted junctions, to the FPS (by the coupling flange) and to the cover head. The volume inside the inner pipe is called Insulation Volume. The outer pipe is welded to the inner pipe in the lower end by a flange which allows a bolted connection between the dead volume and the fitting volume. It extends to the cover gas, above the free level. The annulus between the inner and outer pipes, kept melt-free by design, is linked to the cover gas and filled by a thermal insulator in order to reduce the radial heat flux towards the insulation volume.
- *Decay Heat Removal System*: corresponds to the heat sink of the system in the case of DHR scenario, when the HX is unavailable. It is hydraulically de-coupled by the primary system being placed into the downcomer. The DHR heat exchanger has been designed to have a thermal duty of

40 kW, which represents 5% of the ICE nominal power (800 kW). It is fed by air at atmospheric pressure.

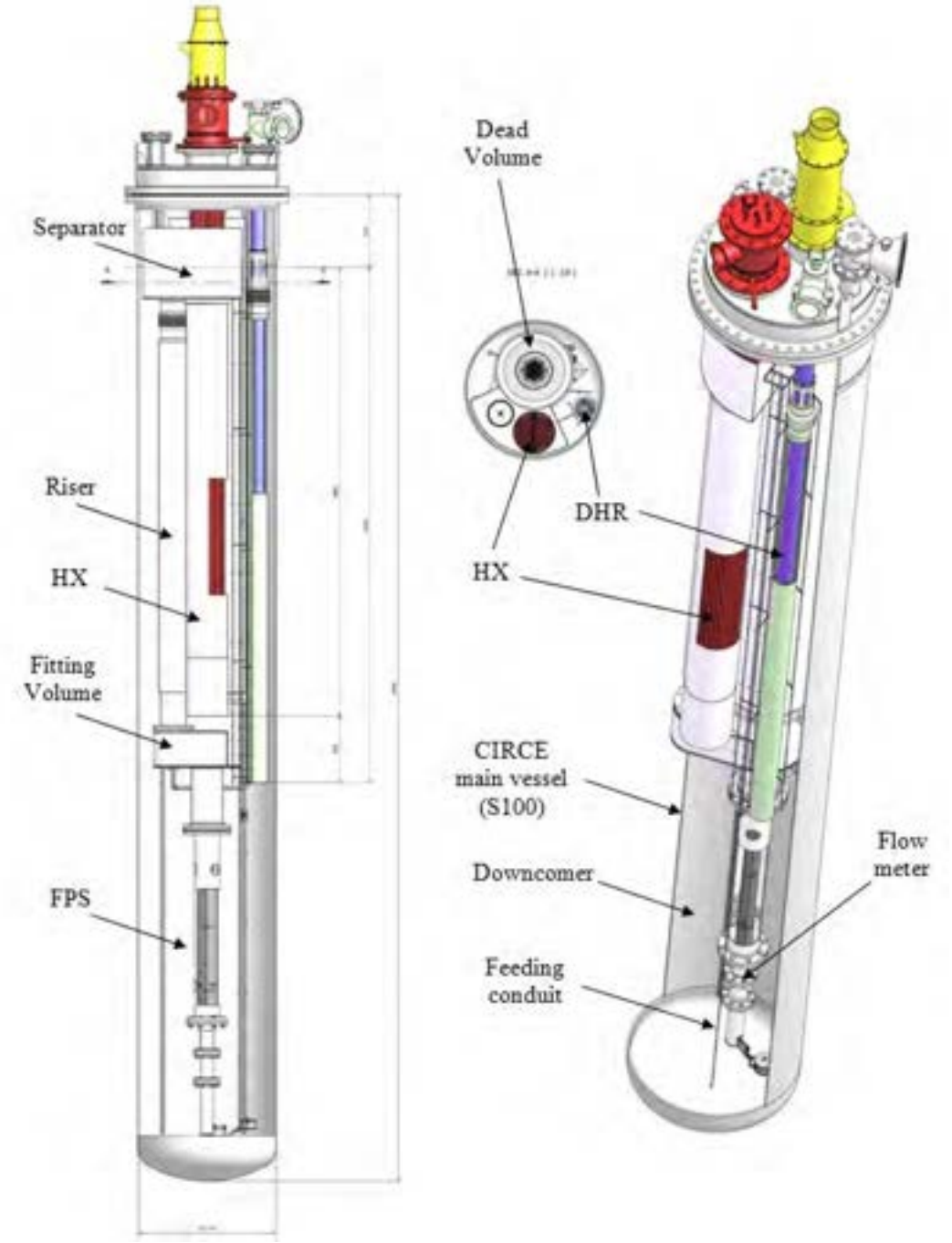

Figure 2 ICE Test section

2. THE FACILITY INSTRUMENTATIONS

In order to investigate the stratification and mixing phenomena in the pool region and the thermal hydraulic behavior of an HLM-cooled rod bundles, all the facility was instrumented with several thermocouples. All thermocouples are N type with isolated hot junction and with an accuracy of ±0.1°C for those installed in the FPS and ±1°C for the others. Moreover, in order to evaluate the mass flow rate through the ICE test section, a Venturi-nozzle flow meter was installed at the entrance of the test section, after the feeding conduit. Finally, once the DHR was activated, the air mass flow rate flowing through the inner pipe of the DHR was measured by a hot wire anemometer.

Instrumentations of the FPS

The ICE Heat Source (HS) consists of an electrical pin bundle with a nominal thermal power of about 800 kW. It was designed to achieve an average LBE velocity of about 1 m/s in agreement with the reference values adopted for LMFR cooled by lead or lead bismuth.

The HS was composed by 37 electrical pins arranged in a wrapped hexagonal lattice (see Figure 3).

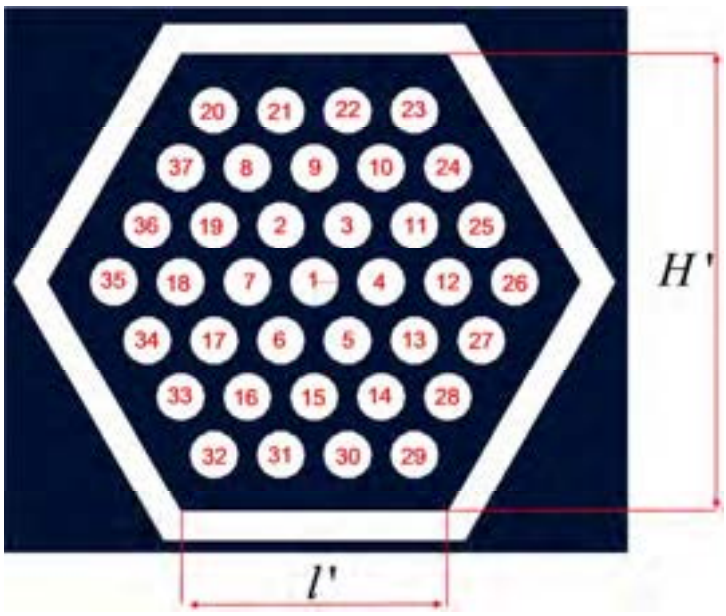

Figure 3: HS cross section (*l'* = 55.4 mm, *H'* = 96 mm)

The relative position between the pin bundle and the wrapper was assured by three appropriately spaced grids (see Figure 4) placed along the axis of the component and fixed to the wrapper. The upper and lower spacer grids were placed at the interface between the active and non-active length of the electrical pins to enclose the mixing zones. The middle spacer grid was placed in the middle section of the bundle active length. From a hydraulic point of view, the FPS assures that the overall LBE flow rate runs along the HS, without any by-pass.

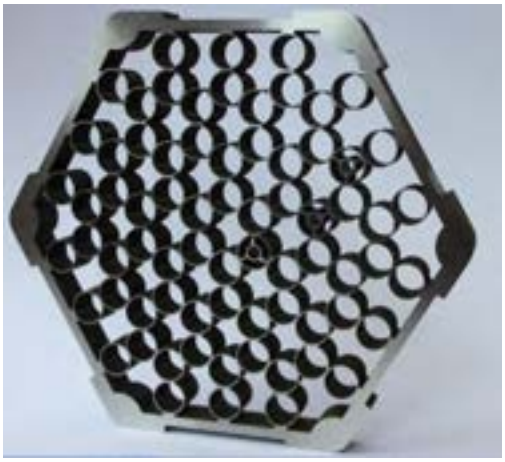

Figure 4: Spacer grid

The LBE temperature at the FPS entrance was measured by three thermocouples with a diameter of 3 mm (TC-FPS-31, 32, 33, see Figure 5). The LBE temperature at the FPS exit section was measured by three thermocouples (TC-FPS-37, 38, 39) of the same type of those at the entrance.

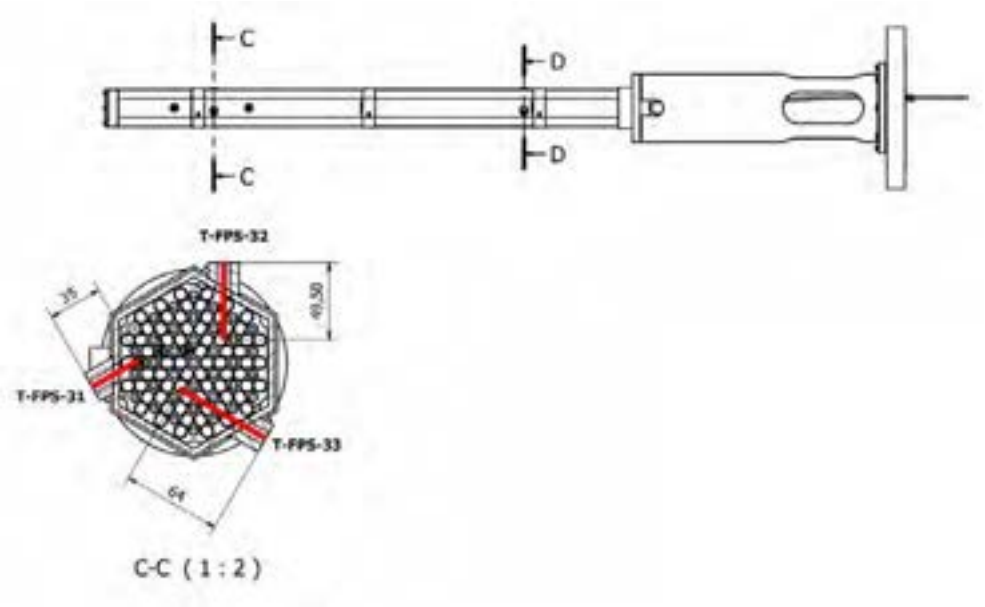

Figure 5: Thermocouples at the FPS entrance

Regarding the positioning of the thermocouples along the FPS active zone, four different sections have been monitored (see Figure 6).

Section 1: 20 mm upstream the middle spacer grid. In this section three different sub-channels have been instrumented (see Figure 7). In each sub-channel both pin clad and LBE bulk temperatures were measured (TC-FPS-01 ... 09)

Section 2: on the matching surface between the middle spacer grid and the fuel pins . In this section the same sub-channels have been identified as in the section 1, aiming at the hot spot factor evaluation due to the installation of the spacer grid itself. In this case only the pin clad temperature was monitored by TCs (TC-FPS-10 ... 14).

Section 3: 60 mm upstream the upper spacer grid. In this section the same sub-channels have been identified in sections 1 and 2 for temperature measurements at the upper height of the bundle. In each sub-channel both pin clad and LBE bulk temperatures were measured by TCs (TC-FPS-16 ... 24).

Section 4: 60 mm downstream the lower spacer grid. In this section the LBE bulk temperature was measured in each sub-channel (TC-FPS-28 ... 30).

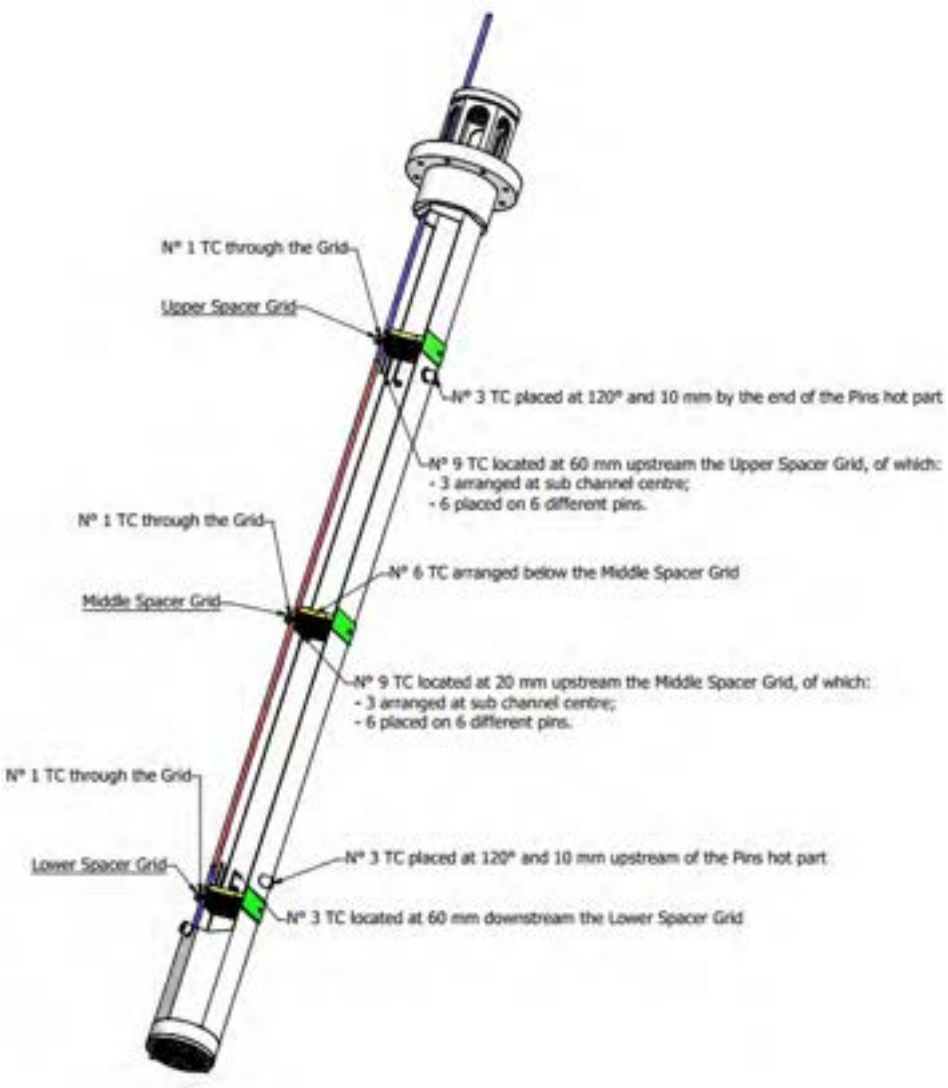

Figure 6: FPS measurement sections

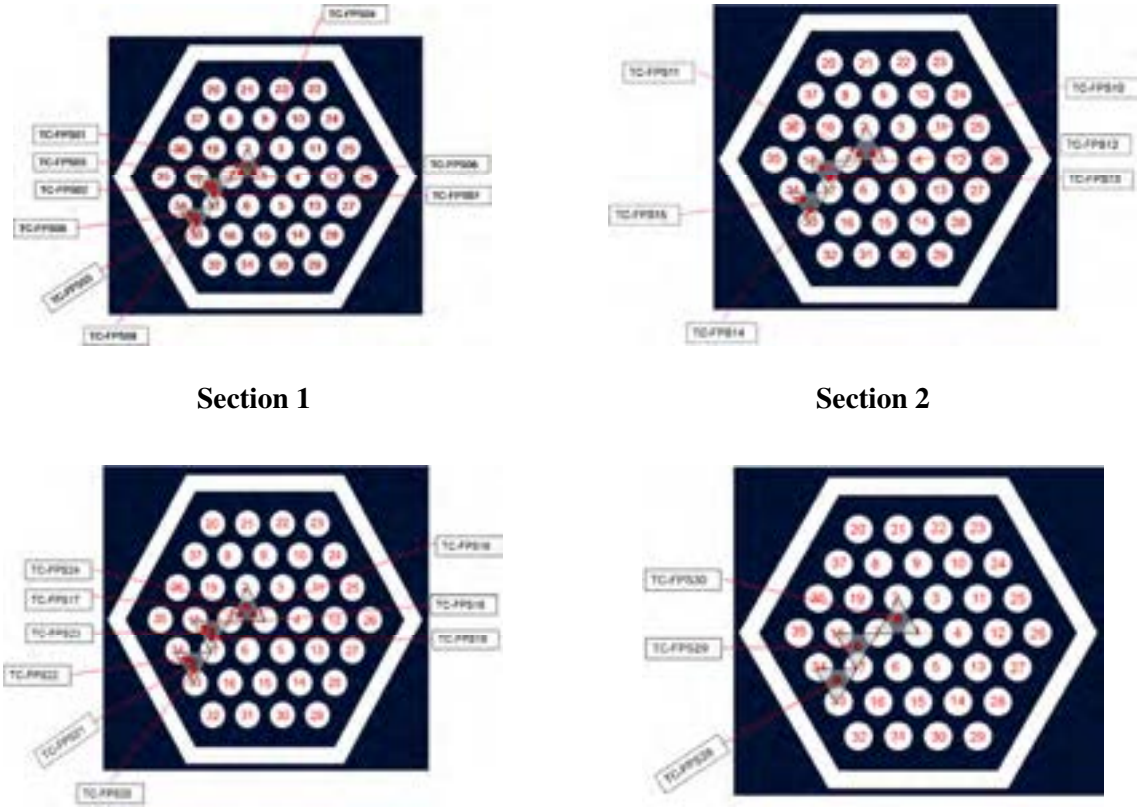

Section 1 **Section 2**

Section 3 **Section 4**

Figure 7: sub-channels instrumented

Thermocouples used in the four sections previously defined have a diameter of 0.5 mm. As previously mentioned, all the thermocouples installed in the FPS were calibrated with an accuracy of ± 0.1 °C.

Instrumentation of the RISER and of the HX

The LBE heated by the FPS flows through the fitting volume into the riser; here temperatures were measured using TCs with a diameter of 3 mm disposed three at the entrance section (T-TS-01 ... 03), and three at the exit section before the separator (T-TS-04 ... 06).

From the riser exit, the LBE flows through the Separator into the HX shell, where the temperatures at the entrance section were measured by three TCs placed at 120°, 30 mm from the bottom of the Separator (T-SG-01 ... 03).

Sub-channel temperature measurements were taken in a plane placed 30 mm above the lower grid, according to the scheme shown in Figure 8 (T-SG-04 ... 12).

Temperatures at the HX exit were measured with six TCs (T-SG-13 ... 18) placed at 60° each and at 100 mm before the HX skirt exit (see Figure 9).

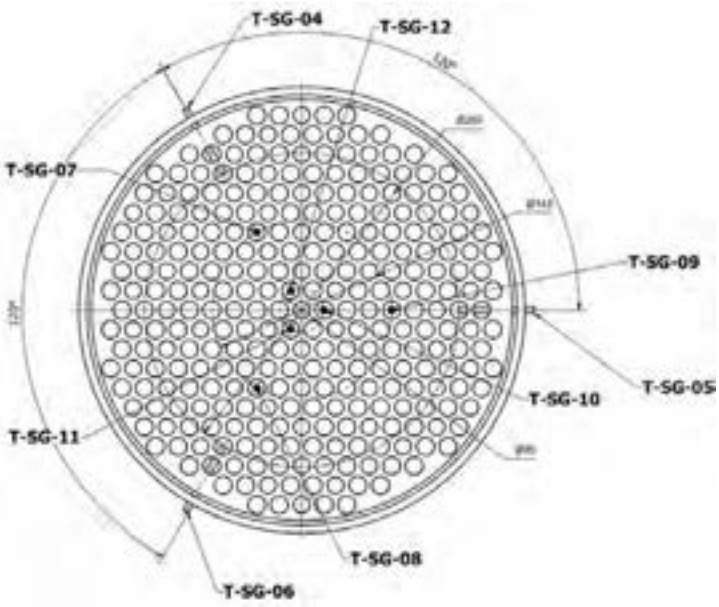

Figure 8: HX Sub-channels TCs configuration

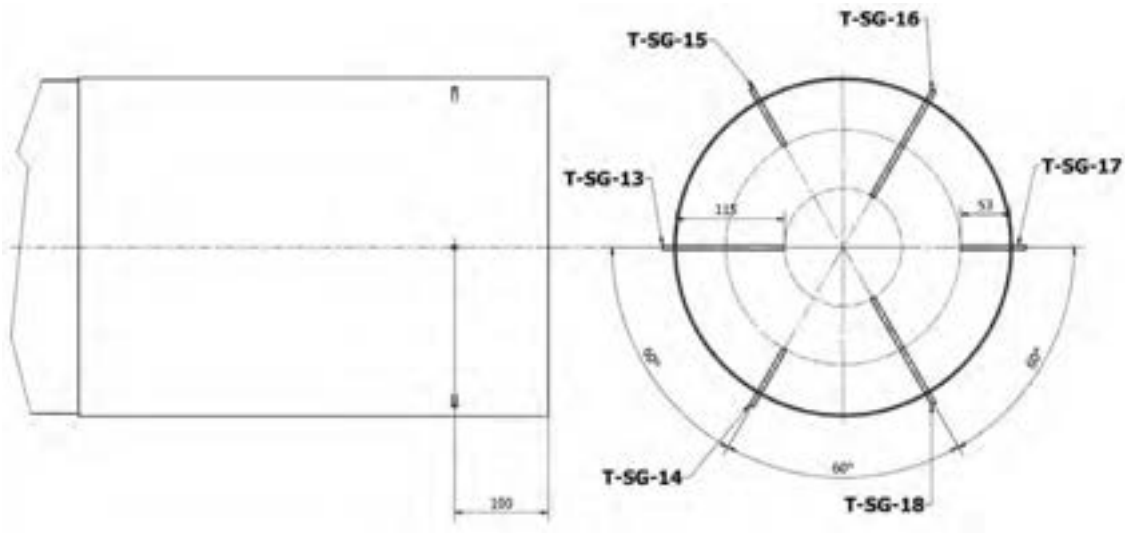

Figure 9: TCs configuration at the HX exit

Instrumentation of the DHR

The Decay Heat Removal system (DHR) is activated to reproduce behavior in case of an accidental event with total loss of HX heat sink and consequent reactor scram [3]. The velocity of the air flowing through the inner tube was measured by a hot wire anemometer placed in the tube at the entrance of the DHR and the mass flow rate was derived using the calibration curve given by the manufacturer. The air temperature was measured at the entrance and at the exit section of the secondary circuit, as shown in Figure 10.

Regarding the primary circuit (LBE side), temperatures at the inlet of the DHR were measured by six TCs with a diameter of 3 mm, placed in the bottom hole at the entrance of the DHR according to Figure 11 (T-DHR-07 ... 12).

The LBE temperature at the exit of the DHR was measured at 60 mm from DHR skirt bottom, by six TCs with a diameter of 3 mm (T-DHR-01 ... 06) placed at 60° according to the scheme showed in Figure 12.

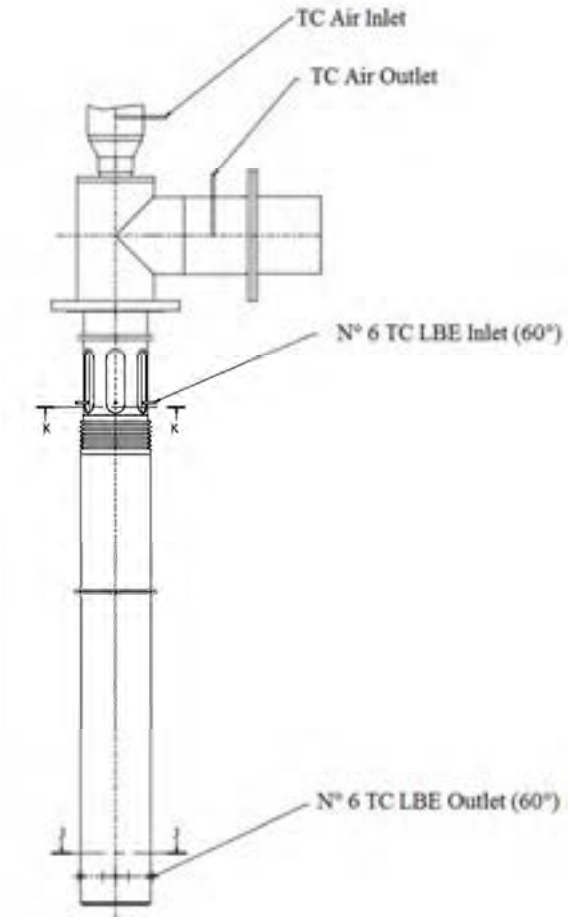

Figure 10: Sketch of TCs placed in the DHR

Instrumentation in the LBE pool

Several TCs were installed into the LBE pool in order to investigate mixing and stratification phenomena. For that pourpose, vertical rods for the TCs attachment have been installed into the pool fixing the TCs at 17 different elevations for a total of 119 TCs with a diameter of 3 mm (T-MS-01 ... 119).

In particular, according to Figure 13, TCs on lines A, H, I allow measurement from the bottom side of the test section up to the FPS entrance, while TCs on lines B, C, D, E, F, G allow measurement up to 600 mm below the exit of the DHR.

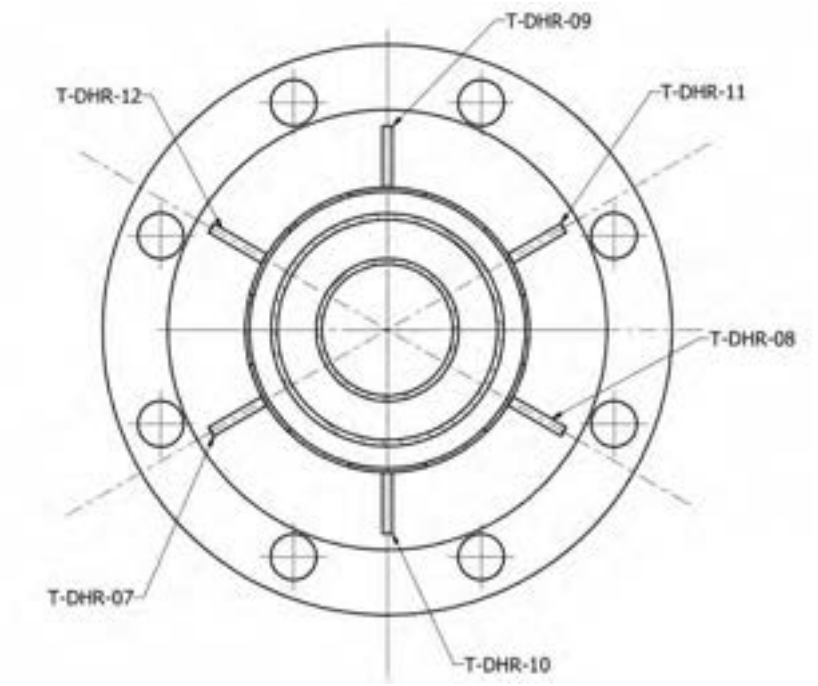

Figure 11: TCs configuration at the DHR inlet

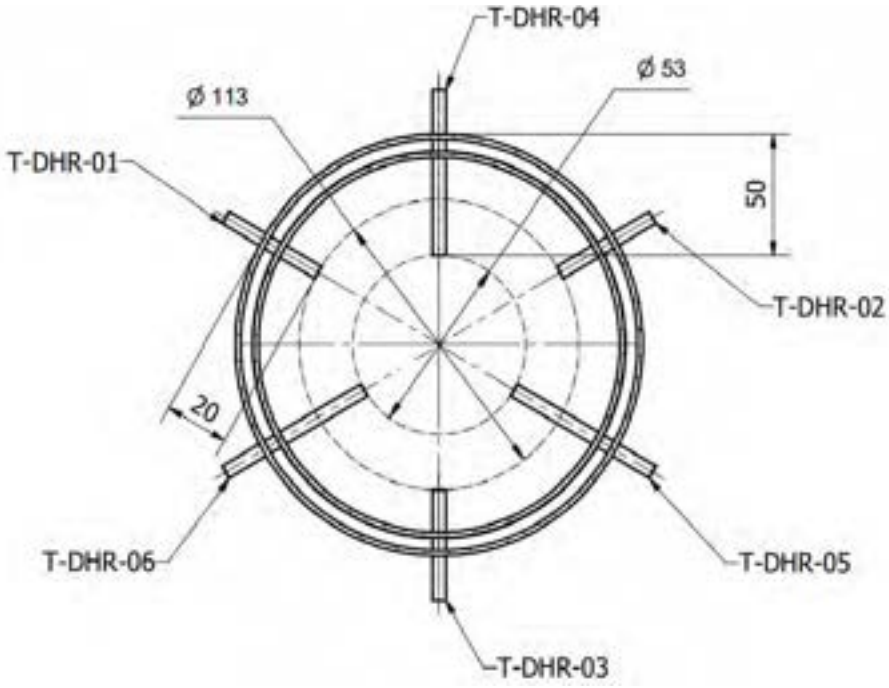

Figure 12: TCs configuration at the DHR outlet

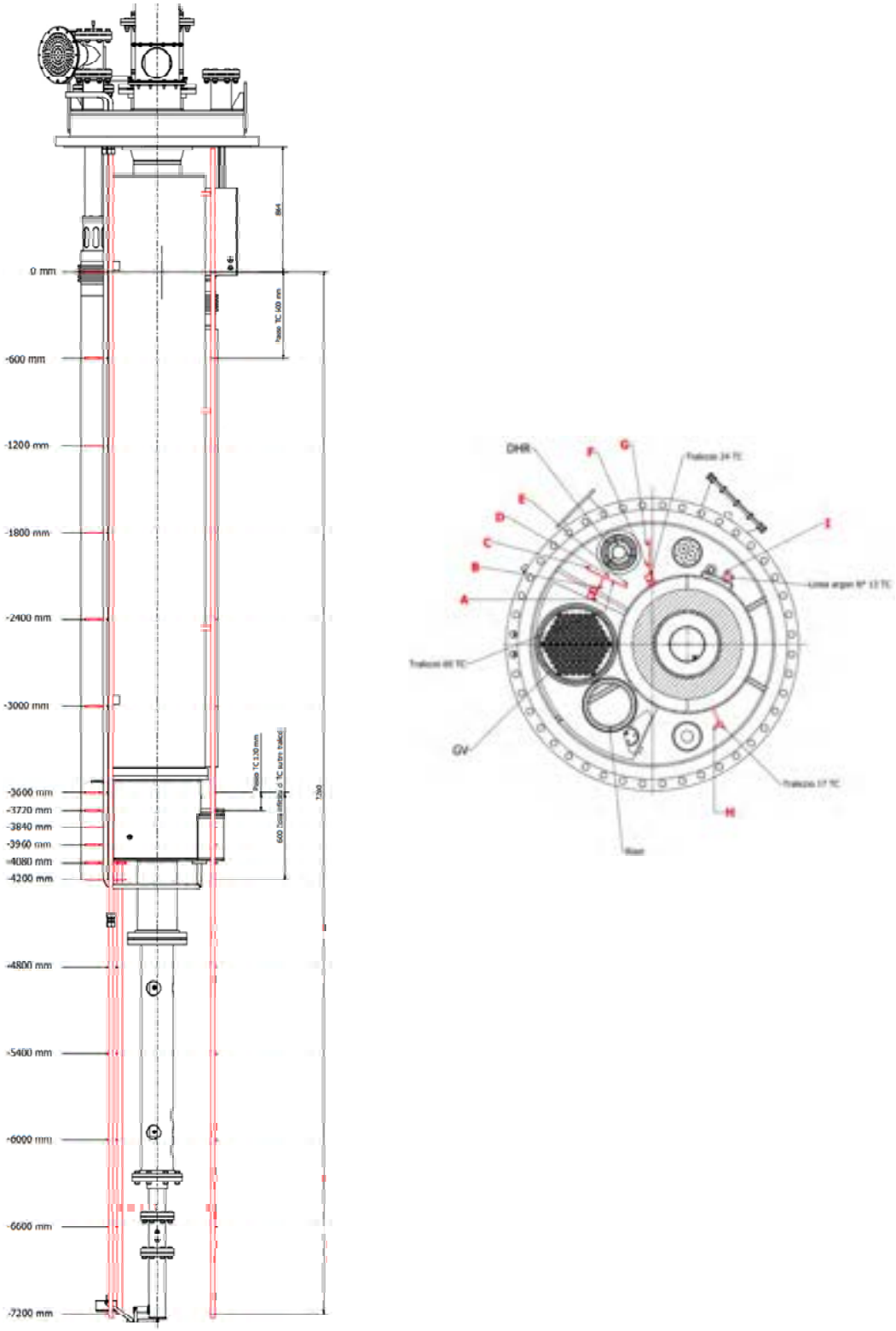

Figure 13: TCs vertical positioning (right) and arrangements of the vertical support (left)

In Table 3 the listed TCs present inside the LBE pool are reported, specifing their name and vertical position.

Table 3: TCs placed inside the LBE pool

TC	*Vertical support*	*Vertical position [mm]*
T-MS-01 to T-MS-05	A,B,C,D,E	0
T-MS-06 to T-MS-07	F,G	
T-MS-08	H	
T-MS-09	I	
T-MS-10 to T-MS-14	A,B,C,D,E	-600
T-MS-15 to T-MS-16	F,G	
T-MS-17	H	
T-MS-18	I	
T-MS-19 to T-MS-23	A,B,C,D,E	-1200
T-MS-24 to T-MS-25	F,G	
T-MS-26	H	
T-MS-27	I	
T-MS-28 to T-MS-32	A,B,C,D,E	-1800
T-MS-33 to T-MS-34	F,G	
T-MS-35	H	
T-MS-36	I	
T-MS-38 to T-MS-41	A,B,C,D,E	-2400
T-MS-42 to T-MS-43	F,G	
T-MS-44	H	
T-MS-45	I	
T-MS-46 to T-MS-50	A,B,C,D,E	-3000
T-MS-51 to T-MS-52	F,G	
T-MS-53	H	
T-MS-54	I	
T-MS-55 to T-MS-59	A,B,C,D,E	-3600
T-MS-60 to T-MS-61	F,G	
T-MS-62	H	

T-MS-63	I	
T-MS-64 to T-MS-68	A,B,C,D,E	-3720
T-MS-69 to T-MS-70	F,G	
T-MS-71	H	
T-MS-72 to T-MS-76	A,B,C,D,E	-3840
T-MS-77 to T-MS-78	F,G	
T-MS-79	H	
T-MS-80 to T-MS-84	A,B,C,D,E	-3960
T-MS-85 to T-MS-86	F,G	
T-MS-87	H	
T-MS-88 to T-MS-92	A,B,C,D,E	-4080
T-MS-93 to T-MS-94	F,G	
T-MS-95	H	
T-MS-96 to T-MS-100	A,B,C,D,E	-4200
T-MS-101 to T-MS-102	F,G	
T-MS-103	H	
T-MS-104	I	
T-MS-105	A	-4800
T-MS-106	H	
T-MS-107	I	
T-MS-108	A	-5400
T-MS-109	H	
T-MS-110	I	
T-MS-111	A	-6000
T-MS-112	H	
T-MS-113	I	
T-MS-114	A	-6600
T-MS-115	H	
T-MS-116	I	
T-MS-117	A	-7200
T-MS-118	H	
T-MS-119	I	

3. EXPERIMENT DESCRIPTION

The experimental tests performed in the frame of CIRCE Experiment were Protected Loss Of Heat Sink (PLOHS) with Loss Of Flow (LOF). The tests were aimed at simulating the total loss of the secondary circuit, the consequent reactor scram and activation of DHR system to remove the decay heat power (5% of the nominal value), in a HLM nuclear system. In the CIRCE-ICE facility the transition from nominal condition (forced circulation) to natural circulation will be run by reducing the thermal power generated in the HS, stopping the argon injection into the riser, cutting off the main HX and activating the DHR heat exchanger. Table 4 summarizes the main nominal parameters that define the accidental scenario experimentally reproduced.

Table 4: Nominal parameters for the experimental campaign

Nominal Steady State	***PLOH+LOF transient***
HS Thermal Power :700-800 kW **HLM flow rate: 55 kg/s (by gas lift)** **ΔT along the HS: 100°C** **Average velocity into the HS:1m/s** **Average temperature along the main flow path: 350°C** **Vessel heating system: not active** **HX flow rate: 0.5 kg/s** **DHR: not active**	Isolation of the main HX (isolating the feed water) Core "scram" at 20-50 kW (decay power) Start-up of the DHR-system ($\dot{m} = 0.3$ kg/s) "Main pump" turn-off (the gas injection is interrupted) Vessel heating system: not-active

4. EXPERIMENT RESULTS (TEST IV)

Figure 14 (a) shows the power transient during the running of Test IV. The experiment starts with nominal power of about 730 kW, and after 7 hours the transition to 50 kW. The primary LBE flow rate, which quickly reaches its nominal value, is about 56-57 kg/s (see Figure 14 (b)); the strong oscillations in the first phase of the test showed in Figure 14 (b), characterized by argon injection assisted circulation, is related to the specific volumetric blowers used to inject the gas into the riser. After a few hours a check valve was put in service to dump such oscillations. After the gas injection switches off and the electrical power supply reduces to about 5% of nominal power, natural circulation conditions establish with the LBE flow rate that tend to about 7.5 kg/s (14% of the nominal flow rate).

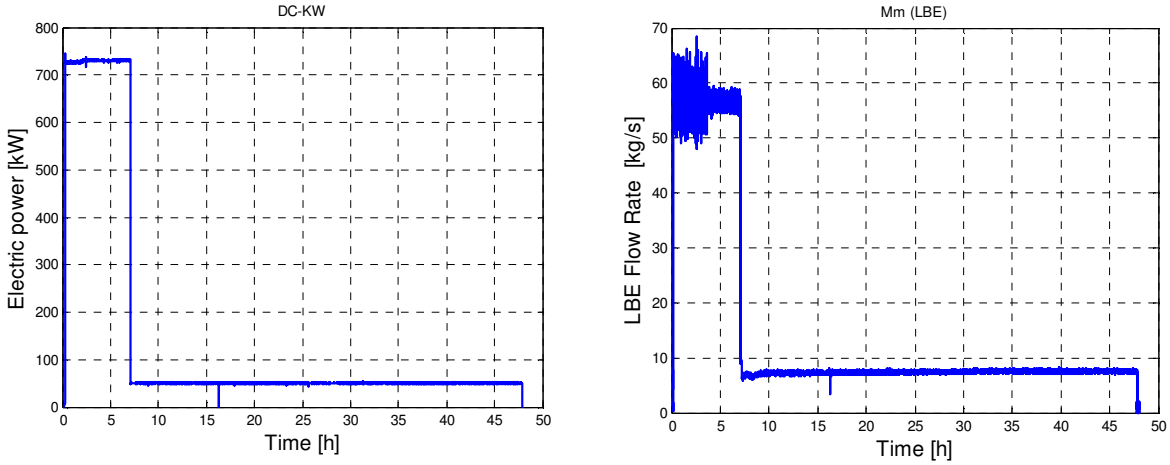

(*a*) (*b*)

Figure 14: Electrical power supplied to the FPS (*a*) and LBE flow rate through the primary system measured by the Venturi flow meter (*b*).

During the full power run, argon is injected into the riser to promote the main circulation along the primary system (gas flow rate of 1.8 Nl/s). After the transition from full power to "decay power", the gas injection was interrupted (see Figure 15 (a)) to simulate the station black-out, and transition from forced to natural circulation takes place. Argon mass flow rate revealed by the trasducer after the injection shutdown shows a value of 0.35 Nl/s, even if the argon line was compleately closed due to the signal being at digital full scale (0.35-3.5 Nl/s). At full power run the HX is fed by water with a flow rate of 0.65 kg/s and water pressure at the inlet of the bayonet tubes (upward the manifold) is close to around 2 bar. After the station black-out simulation conditions the feedwater is closed and the water flow into the HX falls as shown in Figure 15 (b).

After the "core scram", in order to remove "decay heat" power, the DHR-system was activated; the air mass flow rate through the DHR was about 0.223 kg/s, as reported in Figure 16.

Figure 17 shows the average temperatures at inlet and outlet sections of the FPS. As can be noted, steady state conditions were achieved at full power after 4-5 hours of transients with a temperature

difference between the inlet and otlet section of about 77°C, the average inlet temperature being 285°C and the outlet average temperature 362°C.

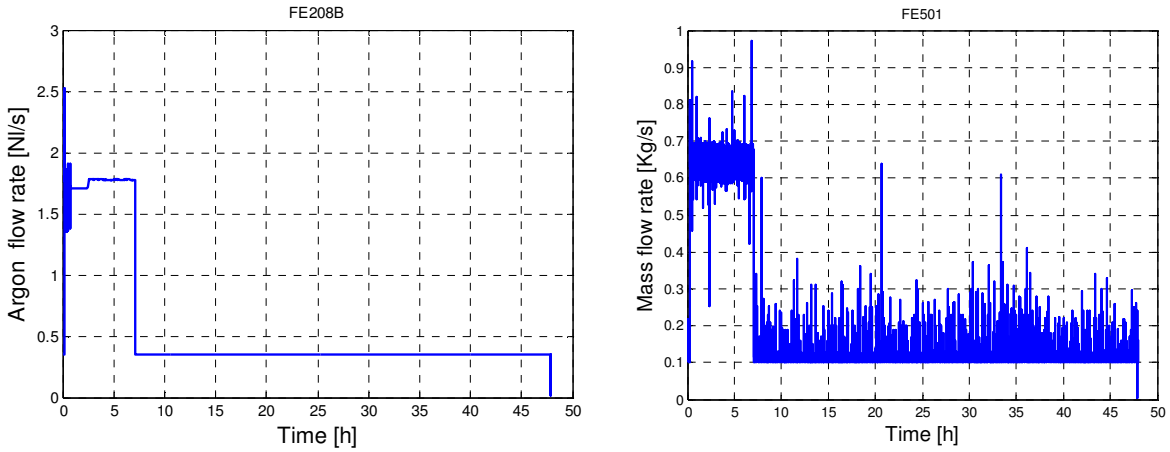

(*a*) (*b*)

Figure 15: Argon flow rate for the gas lift (*a*) and water mass flow rate in the HX (*b*)

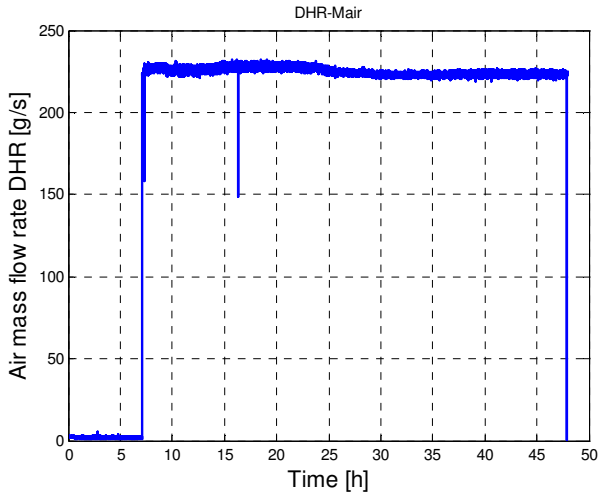

Figure 16: Air mass flow rate through the DHR system

At black-out simulation time, the average temperature at the FPS inlet decreases by about 5°C to a value of about 280°C, while the average temperature of the FPS exit decreases by 70°C reaching a value of about 295°C. Under natural circulation flow regime, the temperature difference along the FPS falls to around 24°C, being the average inlet and outlet temperature 349°C and the average outlet temperature of 373°C, at the end of the test. After a natural circulation transient of about 40 hours, the average temperature in the FPS still increases, and steady state conditions were not yet reached.

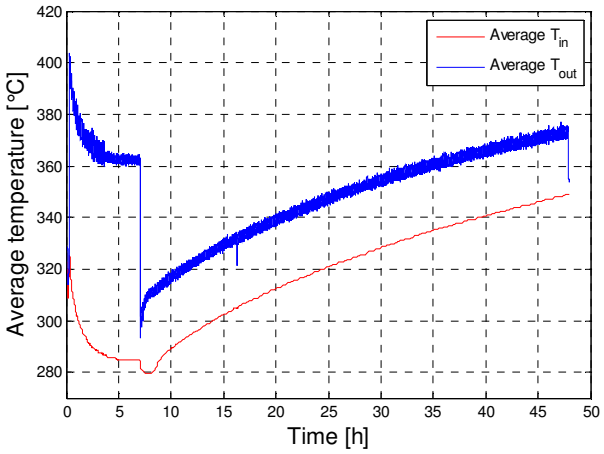

Figure 17: Average temperatures through the FPS

Regarding temperatures in the sub-channels of the FPS at section 1 (placed 20 mm upstream of the middle spacer grid), Figure 18 (a) shows the clad and central channel temperatures in the sub-channel associated to the pins 1-2-7 (Inner sub-channel), while in Figure 18 (b) the temperature difference between the clad average temperature and the temperature in the center of the channel is reported. During full power phase, thermocouples placed on pins 1 and 7 measure temperature values of about 380-390°C, while the thermocouple in the central channel gives a temperature of about 315-320°C.

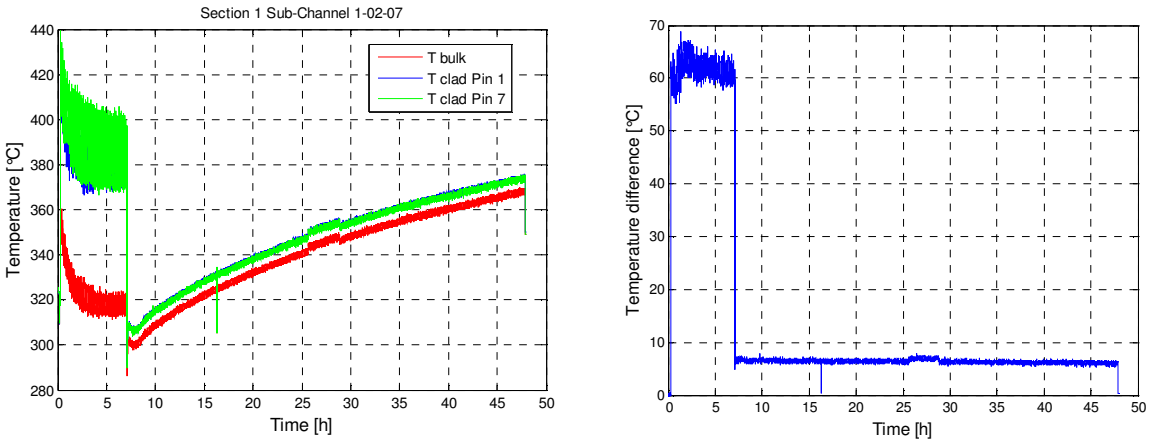

(*a*) (*b*)

Figure 18: Section 1 temperature measurement in the Inner sub-channel (*a*) and temperature difference between the clad average temperature and the center channel temperature (*b*)

After the transition to natural circulation, the temperature on the clad falls to a value between 305 and 310°C while the temperature in the center of the sub-channel falls to about 300°C. At the end of the test, the temperatures reached at the pin walls are about 373°C, while that of LBE at the center of the sub-channel is about 367°C.

The difference between the clad average temperature and the LBE sub-channel central temperature at full power steady state conditions is about 60°C and after the transition to natural circulation this difference falls to a value of about 6-7°C (see Figure 18 (b)).

Considering the sub-channel of the FPS at section 3 placed 60 mm upstream the upper spacer grid, the temperatures at the walls of pins 7 and 1 (Inner sub-channel) reach a value respectively of 430 and 410°C (see Figure 19 (a)). That difference can again be related to non-uniformity of power generation into the electrical heater rods simulating the fuel pins. At the end of the test the pins wall temperatures reach a value of about 395°C, while in the sub-channel center the temperature is about 389°C. According to Figure 19 (b), the difference between the clad average temperature and the center sub-channel temperature is about 53°C at full power and about 6°C after thermal power reduction.

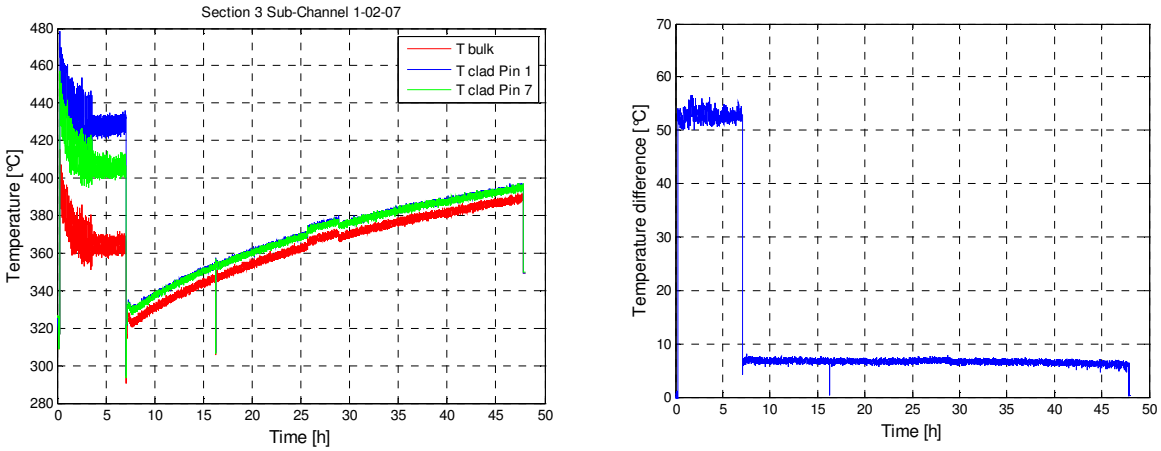

(*a*) (*b*)

Figure 19: Section 3 temperature measurement on the Inner sub-channel (*a*) and temperature difference between the clad average temperature and the center channel temperature (*b*)

Figure 20 (*a*) and (*b*) show the clad temperature of pin 1 and 7 associated with Inner sub-channel along the active length . After about 5 hours the temperature at Section 1 and 2 near the middle spacer grid reaches a constant value of about 380-390°C for pin 1 and 7 (T-FPS 4, 5, 10 and 11), while at section 3 the clad temperature for pin 1 (T-FPS 16) is about 20°C higher than the clad temperature of pin 7 (T-FPS 17, 410°C versus 430°C). After the transition from forced to natural circulation, the clad temperatures increase both for pin 1 and 7, from a value of about 310 to 370°C at Section 1, from 320 to 380°C at Section 2 and from 330 to 395°C at Section 3.

Figure 21 shows the temperature in the center of the channel for the Inner sub-channel. Starting from Section 4 (T-FPS 30, 60 mm downstream of the lower spacer grid), the temperature at full power steady state condition reaches a value of about 280°C, it increases along the sub-channel reaching a value of about 320°C at Section 1 (T-FPS 01) and at Section 3 (60 mm upstream the upper spacer grid) the temperature value is about 365°C (T-FPS 24), hence the LBE flowing in the Inner sub-channel, from Section 4 to Section 3, increases its temperature by about 85°C. After the transition the temperature difference between the lower Section 4 and Section 3 is in the order of 40-45°C.

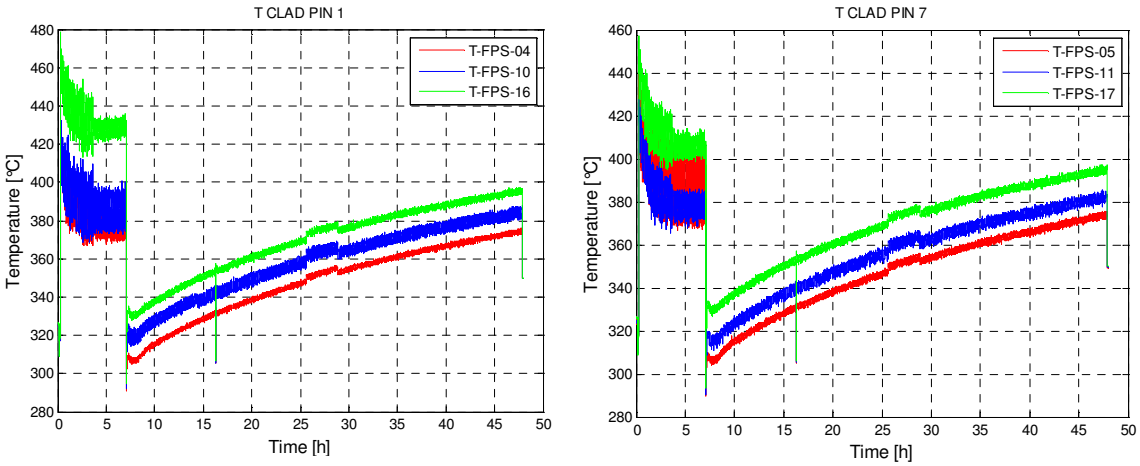

(*a*) (*b*)

Figure 20: Clad temperature pin 1 and 7 along the active length

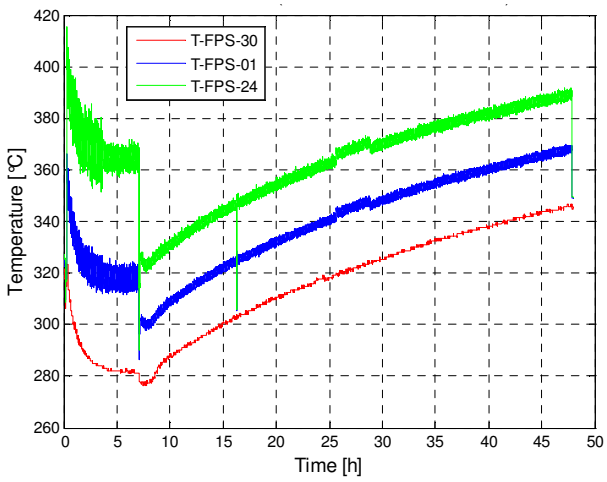

Figure 21: Central sub-channel temperatures

Concerning convection heat transfer into the different analyzed sub-channels at section 1 and 3 the Nusselt number has been calculated according to the following formula:

$$Nu = \frac{HTC \cdot d_{eq}}{k} \qquad (1)$$

where *deq* is the equivalent diameter and, for a triangular array interior channel (assuming an infinite lattice), is evaluated by [12]:

$$d_{eq} = 4\frac{\left(\frac{\sqrt{3}}{4}\cdot p^2 - \pi\cdot d\right)}{\frac{\pi\cdot d}{2}} \qquad (2)$$

The heat transfer coefficient is calculated by the Newton relationship *HTC=q''/(Tc-Tb)*, where *q''* is the heat flux, *Tc* and *Tb* are respectively the clad and bulk (the last one is approximated with the temperature at the center of the subchannel) temperatures.

Considering the Inner sub-channel of the FPS, the Nusselt number has been calculated on Section 1 (see Figure 22 (a)) and Section 3 (see Figure 22 (b)) assuming as clad temperature the average temperature between pin 1 and pin 7.

As can be noted, the Nusselt numbers at Section 1 and 3 are, as expected for a fully developed flow, in agreement both under forced and natural circulation (going from 21-24 under forced circulation to 13-14 under natural circulation). Moreover, the Nusselt number during the transients soon reaches an asymptotic condition, although the average temperature of the system rises due to the global thermal unbalance.

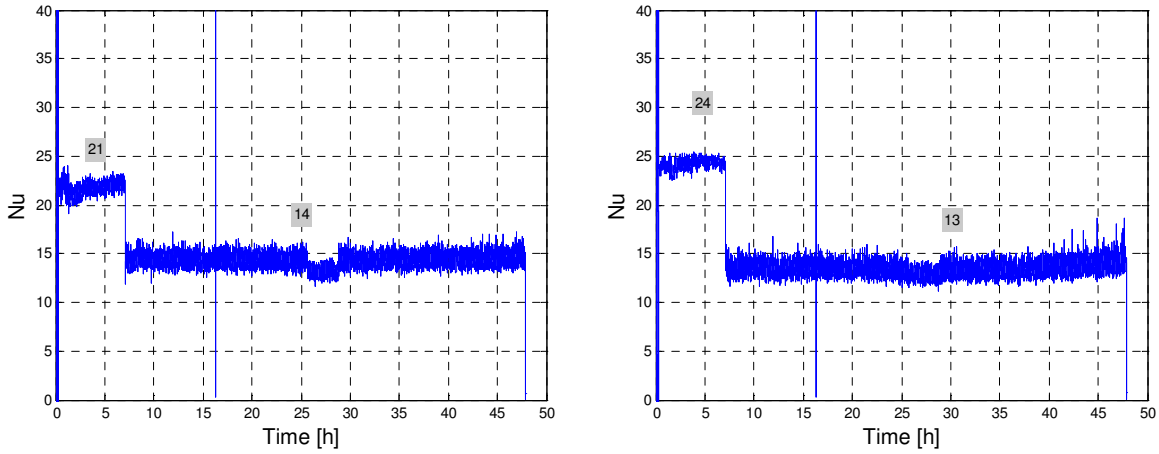

(*a*) (*b*)

Figure 22: Nusselt number in Section 1 (*a*) and in Section 3 (*b*) evaluated into the Inner sub-channel averaging the clad temperatures.

In the following the average experimental Nusselt number is compared with the correlations of Ushakov (Eq. 3), Mikytiuk (Eq. 4) and Gräber (Eq. 5) [13-16] valid for triangular lattice bundle without spacer grids:

$$Nu = 7.55\cdot(p/d) - 20\cdot(p/d) - 0.041\cdot(p/d)^{-2}\cdot Pe^{(0.56+0.19\cdot p/d)} \qquad (3)$$

valid for $1.2 \le p/d \le 2$ and for $1 \le Pe \le 4000$

$$Nu = 0.047 \cdot \left(1 - e^{-3.8 \cdot (x-1)}\right)\left(Pe^{0.77} + 250\right) \quad (4)$$

valid for $1.1 \le p/d \le 1.95$ adn for $30 \le Pe \le 5000$

$$Nu = 0.25 + 6.2 \cdot x + \left(0.032 \cdot x - 0.007\right) \cdot Pe^{0.8 - 0.024 \cdot x} \quad (5)$$

valid for $1.25 \le p/d \le 1.95$ adn for $110 \le Pe \le 4300$

Figure 23 (a) and (b) compare the Nusselt number computed from the experimental data with the one obtained from the correlations given in Eqs. from (3) to Eq. (5). The average Nusselt number is plotted as a function of the Peclet number.

As observed in Figure 23, under forced circulation regime the Nusselt number assumes a value about 25% lower than that expected from the considered correlations at Section 1 and values about 10-14% lower than that expected from the correlations at Section 3. For the Peclet computation, the calculated average velocity in the core region is about 0.91 m/s (Re = 114720) obtaining a Peclet number in the order of about 2380. After the transition from forced to natural circulation, the Nusselt number underestimates the values obtained from correlations of about 6-26 % (depending from the sub-channel) at Section 1, while at Section 3 the obtained values in the Inner sub-channel underestimates the value obtained from correlations of about 8% while the Nusselt obtained for the Middle sub-channel overestimates that computed from the correlations of about 33%. The calculated average velocity in the core under natural circulation condition is about 0.12 m/s (Re = 15363) obtaining a Peclet number in the order of about 300.

Averaging the Nusselt values obtained in Section 1 and 3, a mean value for the FPS was obtained (see Figure 24).

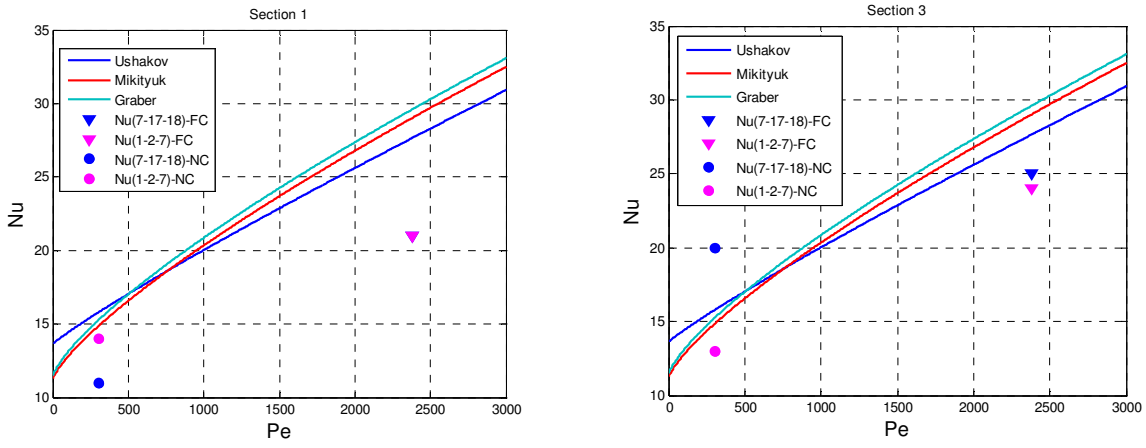

(*a*) (*b*)

Figure 23: Nusselt vs Peclet in Section 1 (*a*) and in Section 3 (*b*)

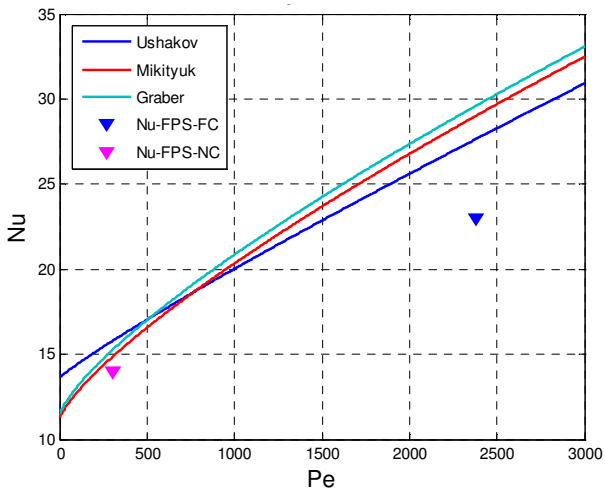

Figure 24: Average value of Nusselt number at Section 1 and Section 3 vs. Peclet number

The Nusselt value obtained from the experimental data underestimates the value calculated using the correlations of a value about 17% under forced circulation conditions and of about 6% under natural circulation conditions.

Inside the Riser, tubes, injecting argon below the liquid metal level, in short "bubble tubes" (accuracy ± 1 mm LBE), have been installed to transfer pressure signals from the LBE alloy to differential pressure cells operating with gas at room temperature. The distance between the entrance of the two bubble tubes into the Riser is hr = 3.6 m computed considering the differential pressure measured before the gas injection and the FPS activation when the LBE is at rest.

Figure 25 (a) shows the differential pressure along the Riser. During forced circulation condition, inlet and outlet pressure difference inside the riser is lower than that measured under natural circulation condition, essentially for the lower value of the two phase flow density compared to the LBE density. In particular, at full power steady state condition the pressure difference reaches a value of about 3420 mbar while, after the transition, the reached value is in the order of 3670 mbar. The pressure drop into the Riser can be obtained as the sum of three components, due to acceleration, friction and gravity

$$\Delta P = \Delta P_{frict} + \Delta P_{acc} + \Delta P_{grav} \qquad (7)$$

and considering that that $\Delta P_{grav} >> \Delta P_{frict} + \Delta P_{acc}$, it is possible to approximate the pressure losses in the Riser with the pressure losses due to gravity. Then, it is possible to evaluate the void fraction in the Riser by:

$$\bar{\alpha} \cong \frac{\rho_{LBE} - \bar{\rho}_m}{\rho_{LBE} - \bar{\rho}_g} \qquad (8)$$

where $\bar{\rho}_m = \frac{\Delta P_m}{g \cdot h_r}$ and $\bar{\rho}_g$ is average gas density in the considered part of the Riser.

Figure 25 (b) shows the mean void fraction along the riser as a function of time for the gas enhanced circulation transient. The obtained value of the void fraction (computed after the check valve has been put in service to lower the oscillations) is about 9%.

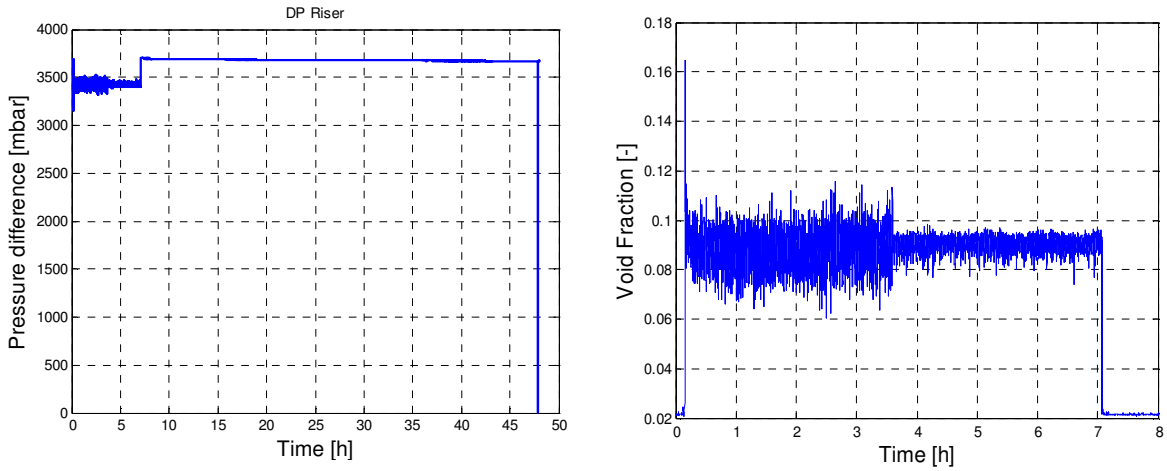

(*a*) (*b*)

Figure 25: Pressure difference between inlet and outlet section of the Riser(*a*) and Void fraction (*b*)

From the riser exit, the LBE flows through the separator into the HX shell. Figure 26 (a) and (b) show HX inlet and outlet temperature, respectively.

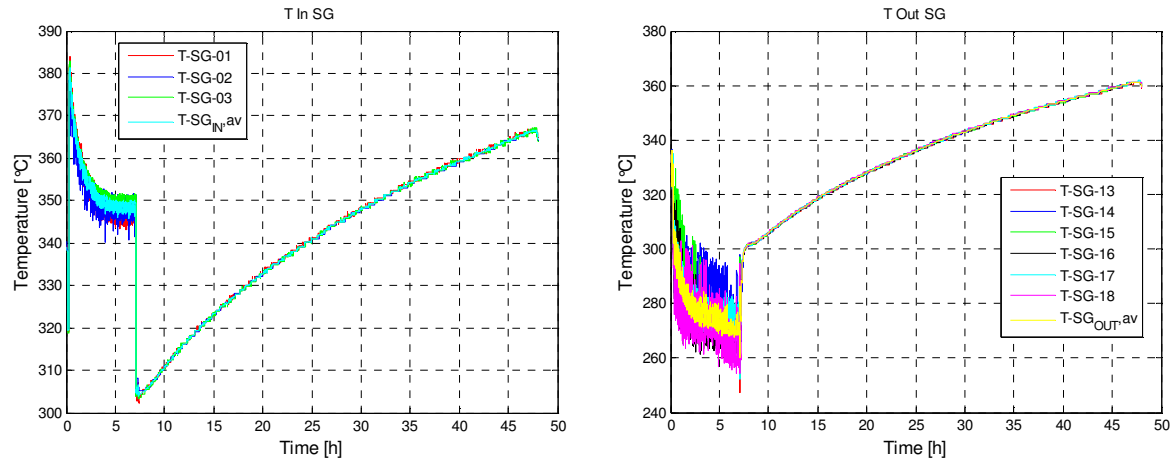

(*a*) (*b*)

Figure 26: LBE temperature at the entrance (*a*) and exit of the HX (*b*).

At full power steady state condition (when the HX is activated) the LBE temperature at the entrance of the HX is about 348°C, then through the HX the LBE exchanges heat with water of the secondary circuit decreasing its temperature by about 78°C reaching at the exit of the HX the value of about 270°C. Immediately after the transition to natural circulation the LBE enters the HX with a temperature of 305°C and exits with a temperature of 301°C, while at the end of the experiment the LBE temperature at the HX inlet section is about 366°C. The temperature drop between the HX inlet

and outlet section under natural circulation condition is 4-5 °C and it is mainly due to heat losses toward the LBE external pool.

Figure 27 shows the thermal power removed by the HX computed from the energy balance equation applied to the LBE side of the HX. At steady state full power conditions the thermal power removed by the HX is in the order of 640 kW.

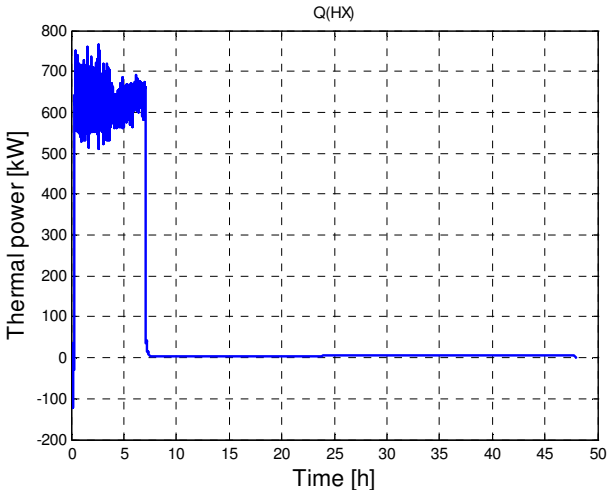

Figure 27: Thermal power removed by the HX secondary side.

The difference between electric power supplied to the FPS and the thermal power removed by the HX at full power steady state condition is essentially due to:

- about 5% of the supplied electrical power converted to heat in the electrical cable for Joule effect and removed by IVCS;
- The calculation does not take into account the power removed by the HX tubes inside the separator before the inlet in the HX pipe;
- Heat losses towards the external environment.

Temperatures at the entrance and exit of the DHR (see Figure 28 (a) and (b)) are now considered.

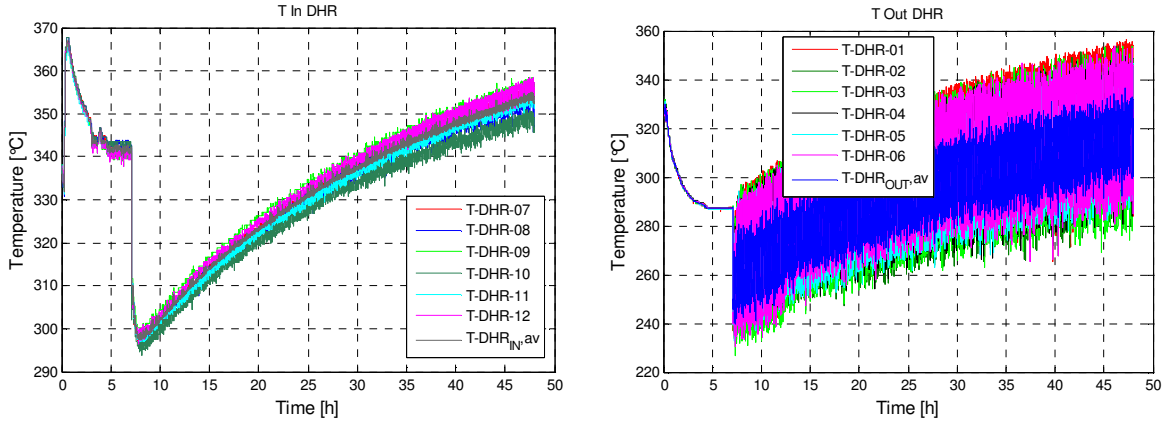

(*a*) (*b*)

Figure 28: LBE temperature at the entrance (*a*) and at the exit (*b*) of the DHR.

After the DHR activation (transition to natural circulation), the temperature at the entrance is about 298°C and gradually increases reaching a value of about 354°C at the end of the test. Regarding the

temperature at the exit of the DHR, after the transition, temperature oscillations of about 50°C are detected. This anomaly is not observed from TCs displaced in the pool next to the exit and its understanding requires further experimental investigation.

When the DHR was activated, the LBE mass flow rate through the DHR sub-channel, quickly reaches a steady state value of about 4 kg/s. LBE mass flow rate through the DHR annular channel is computed from the energy balance equation obtained equating the thermal power transferred from the LBE during the flowing in the LBE annular region, to the thermal power removed by the secondary air side.

For the DHR secondary side, the air mass flow rate is approximately 0.223 kg/s (see Figure 16). The temperature difference between the air inlet and outlet section is about 100àC, while the thermal power removed by the air secondary side computed from the energy balance equation is 23-25 kW.

Inside the external LBE pool, several TCs were installed in order to investigate mixing and stratification phenomena. Figure 29 and Figure 30 shown the temperature inside the LBE pool along the 8 different vertical lines (see Figure 13). In particular TCs on lines A, H, I allow measurement from the upper section (0 mm in Figure 13) to the FPS entrance level (-7200 mm), while TCs on lines B, C, D, E, F, G allow measurement up to 600 mm below the exit of the DHR.

Considering various horizontal sections of the pool (different vertical positions), it is clear, by observing Figure 29 and Figure 30, that the LBE temperature is homogenous at each horizontal section, i.e. the temperature monitored at a certain height behind the dead volume is the same as that monitored near the DHR at the same height.

The temperature in the pool (320-330°C) at the beginning of the experiment is vertically quite uniform changing about 10°C from the first upper TC and the bottom one (7.2 m lower than the first TC).

After about 6 h (see Figure 29), just before transition to natural circulation, with thermal power at steady state condition and a constant Argon mass flow rate (1.78 Nl/s), the LBE temperature in the lower region of the pool is at its coldest assuming a uniform temperature of about 283°C. Between the exits of the DHR and the HX, respectively 4.2 and 3.6 m, a thermal stratification phenomenon with a temperature variation of about 17°C can be observed. In the upper part of the plenum then the temperature increases reaching a value of about 340°C.

After the transition from forced to natural circulation, the supplied electrical power is reduced to 50 kW, the secondary air system in the DHR is activated and the Argon injection is stopped.

The LBE temperature in the upper plenum became uniform and the region where thermal stratification phenomena are significant moves downwards starting from the DHR outlet section. In the lower plenum of the pool the LBE temperature become quite uniform too.

From the transition to t = 47.8 h, temperatures in the pool gradually rise reaching, by the end of the experiment, a value of about 360°C in the upper plenum of the pool and about 350 °C in the lower plenum (steady state condition not yet reached). The temperature difference, in the area where thermal stratification phenomena are relevant, comes down to a value of about 10°C (see Figure 30).

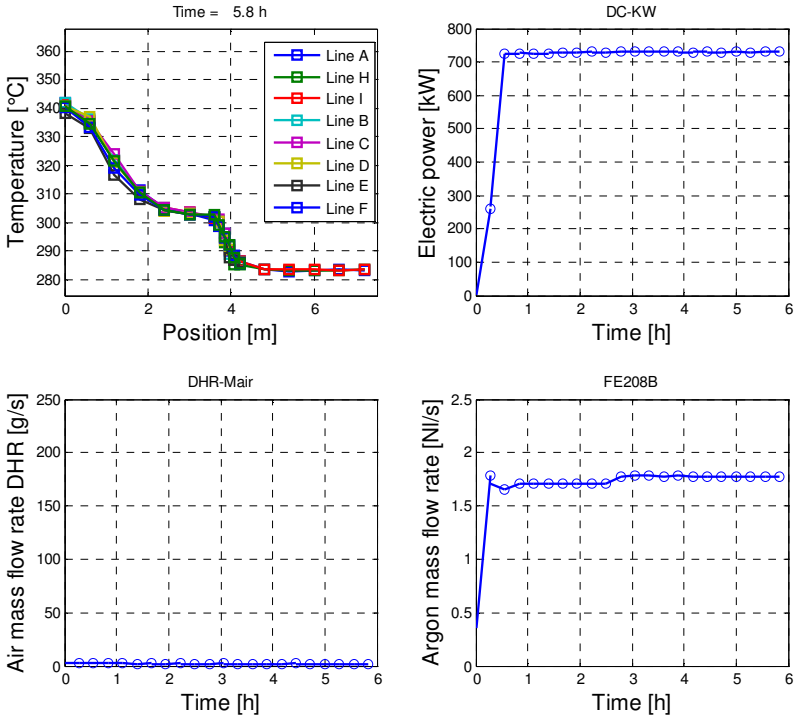

Figure 29: Temperature of the LBE inside the pool at *t* = 5.8h, together with time trends of electrical power, air mass flow rate and argon mass flow rate.

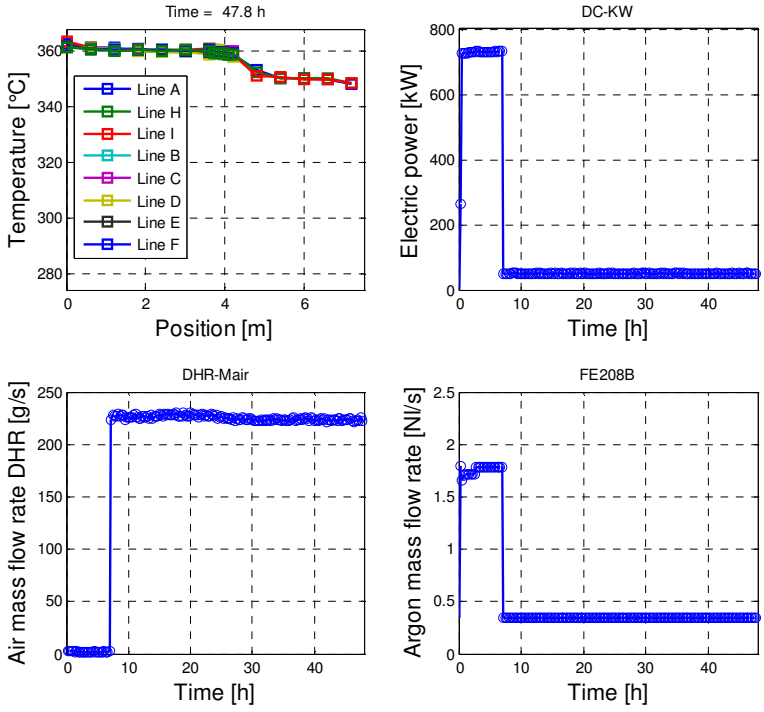

Figure 30: Temperature of the LBE inside the pool at *t* = 47.8h, together with time trends of electrical power, air mass flow rate and argon mass flow rate.

5. TEST IV POST TEST NUMERICAL SIMULATION

In order to assess the RELAP5 prediction capability, a post-test simulation has been performed on TEST-IV of CIRCE facility experiments reproducing an accidental event with total loss of secondary circuit followed by reactor scram and DHR system activation to remove the residual heat generation. The test is representative of a protected loss of heat sink scenario combined with the loss of flow in the primary circuit (PLOH+LOF).

The transition from forced to natural circulation in the primary system has been investigated.

The RELAP5 code [17], conceived to simulate accidental thermal-hydraulic transient in LWR, has been implemented with lead ally thermo-physical properties by the DICI of Pisa University for LBE and lead cooled fast reactors applications. The RELAP5 nodalization scheme used for CIRCE experiments simulations, is depicted in Figure 31.

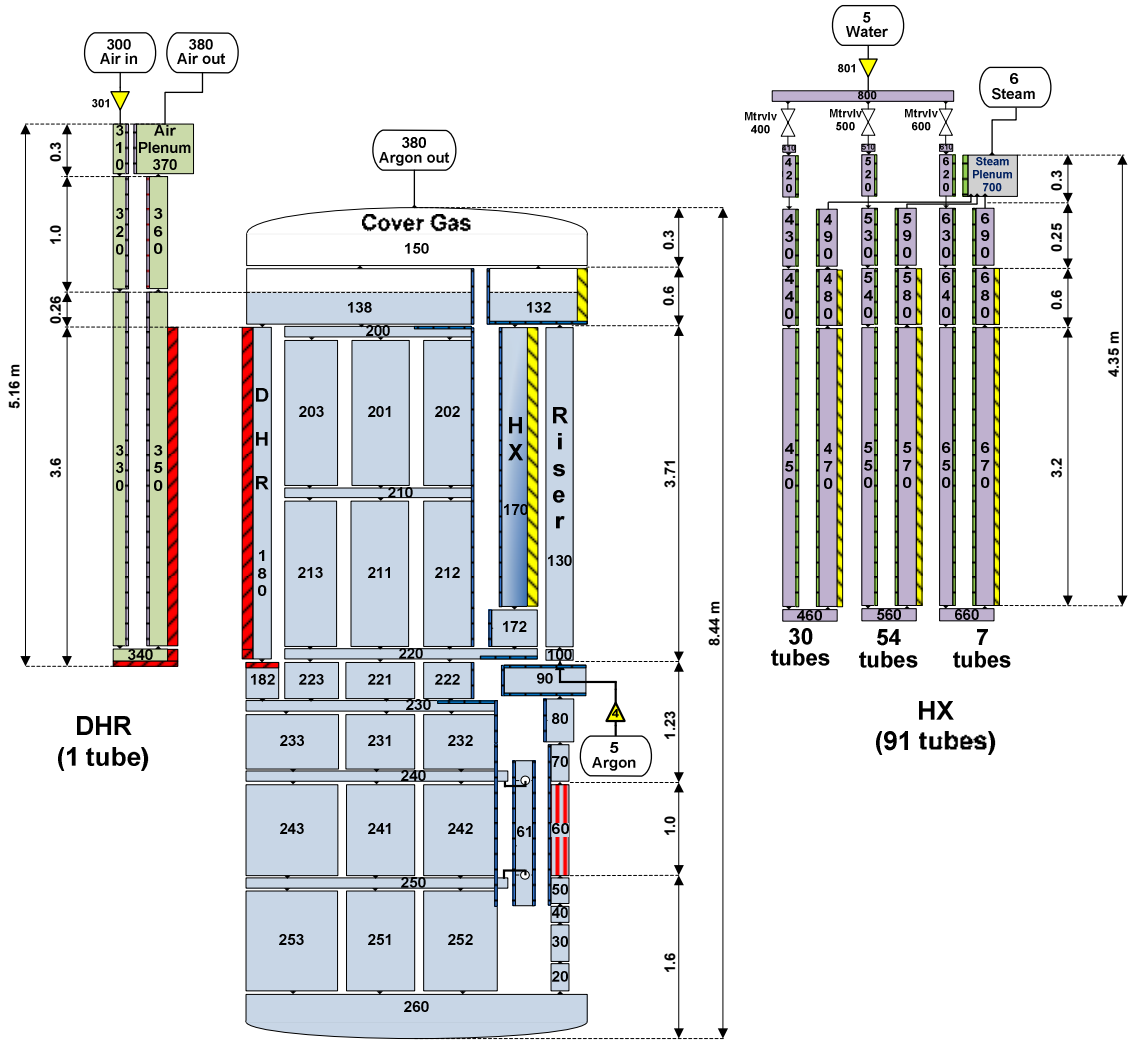

Figure 31: RELAP5 nodalization scheme of CIRCE facility

The upgraded configuration of CIRCE-ICE test section has been modeled.

The main tank S100 contains about 69 tons of primary LBE with an uniform initial temperature of 320°C; the liquid metal level is set to 0.26 m above the Riser outlet. The LBE enters into the aspiration duct from the pool bottom, reaching the Fuel Pin Simulator bundle (FPS), where it is heated (1 m active length, Pipe-60); it then flows upstream, crossing the fitting volume (Pipe-90), through the Riser (Pipe-130) and reaches the separator located in the upper part of the facility. A Time dependent junction (Tmdpjun-4) is connected to the Riser inlet (Branch-100) and injects Argon (from Tmdpvol-4) to simulate the gas lift system during the assisted circulation phase. In the Separator (Branch-132), the gas is separated from the liquid metal and goes up in the vessel cover gas plenum (Branch-150), while the hot LBE goes downwards through the main Heat Exchanger (HX) shell (Pipe-170), to be cooled by the HX secondary water. The LBE exits flowing through a flow straightener (Pipe-172), placed in the lower part of the shell, into the downcomer.

The pool external zone (Pipe/Branch from 200 to 260) has been modeled by means of a series of parallel pipes connected by branches; such a nodalization of the pool, aims at improving the simulation of LBE mixing and thermal stratification phenomena observed experimentally.

The DHR primary side consists in an annular channel region modeled by Pipe-180. During the DHR activation, the hot LBE flows downwards from the pool top region (Branch-138) through the DHR primary side annular channel (Pipe-180). Here, LBE is cooled by the secondary side air flowing upstream through the DHR internal pipe, in a counter current heat exchanger configuration. The LBE cooled by the DHR exits in the pool through the DHR skirt (Pipe-182). Heat generation inside the FPS is simulated by an average heat structure representing the 37 electrical pins; the convective boundary condition is set according to Ushakov correlation [15] for rod bundle.

Similarly, the same correlation is used for the HX primary side convective heat transfer with the 91 tubes.

Heat transfer of LBE from the main flow-path to the quasi-stagnant LBE inside the pool has been considered as well, with the exception of the Riser and the DHR shell which are thermally insulated, therefore considered adiabatic in the simulations.

Heat dispersion of the LBE inside the tank towards the containment building has been taken into account introducing an air convective heat transfer coefficient around 1.5 W/(m^2K).

Pressure losses along the main flow path have been taken into account introducing concentrated pressure losses coefficients to simulate the presence of the Venturi nozzle (placed to measure the LBE flow) and the spacer grids.

The HX secondary side is modeled by three water loops, simulating the three compartments of 7 (inner), 54 (middle) and 30 (outer) bayonet tubes in which the HX bundle is arranged. Water is injected (Tmdpjun-801) inside each loops through three Motor Valves, flows downwards into the inner pipe and rises up through the annular region, where it exchanges heat in counter current with the primary LBE. Along the annular zone length, water begins to change its phase and the water/steam mixture is finally collected in the Steam Plenum (Pipe-700).

The secondary side is thermally coupled with the primary side by means of an adequate heat structures between the water/steam mixture inside the annular zone and the LBE flowing through the tubes

bundles; a cylindrical double wall with helium inside the gap has been modeled to compute the heat conduction. Vertical bundle without crossflow (with a p/d=1.32) convective condition type is set for the right boundary condition (LBE side), whereas the default convection condition is set for left boundary conditions (water/steam). A heat structure is foreseen to take into account the heat transfer between the cold water flowing in the inner tube and the water/steam mixture flowing through the annular zone.

The bayonet tube of the DHR secondary side system is simulated according to the design parameters. The air mass flow rate is imposed at the inner tube inlet section by means of a Time Dependent Junction (Tmdpjun-310); air goes down towards the tube bottom plate and then flows upwards through the annular region up to the air Plenum located above the tank S100 cover. As for the HX, a heat structure provides the thermal coupling of the primary and secondary fluids of the DHR system. Heat transferred between inner tube and annular region, is taken into account as well.

TEST IV. Initial and Boundary Conditions

Test IV starts with CIRCE facility maintained at isothermal conditions (320°C) by means of the heaters which compensate the heat losses. In Figure 32 are illustrated the boundary conditions used for TEST IV.

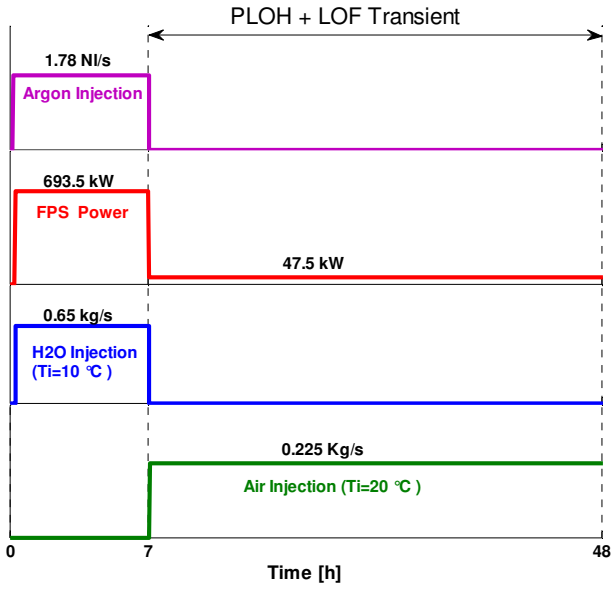

Figure 32: Boundary condition for TEST IV

The RELAP5 simulation post-test analysis reproduces the experimental actions sequence performed during Test IV; the main boundary condition (FPS power, Argon flow, and secondary fluid mass flow rates) are taken from the experimental outcomes. Namely, the simulation begins with the injection of argon (approximately 1.78 Nl/s) inside the Riser to enhance the primary LBE circulation. After

reaching a stabilized value of the primary flow, power is supplied (power ramp) to the FPS up to a nominal value of 693.5 kW.

Simultaneously, the main Heat Exchanger is activated injecting 0.65 kg/s of water inside the 91 bayonet tubes in order to remove the supplied thermal power. This condition is maintained for several hours in order to attain a well stabilized condition in the primary system before the beginning of the transient phase. After about 7 hours from the beginning, the PLOHS+LOF transient is initialized performing the following procedures:

- switching off the gas injection (LOF);
- rapidly reducing the FPS power down to 7% of the nominal value (47.5 kW) representative of the decay power level;
- stopping the HX water injection;
- starting the forced circulation of air (0.225 kg/s) in the secondary side DHR heat exchanger to remove the decay power.

The transient phase goes on for about 40 hours.

TEST IV PLOH+LOF Simulation Analysis

Post-test main outcomes of PLOH+LOF transient are compared with RELAP5 results. Figure 33 show test boundary conditions (namely FPS Power, Argon Flow, HX feedwater and DHR Air Flow) and how they are reproduced in RELAP5 calculation.

FPS Heat Power supply in RELAP5 simulation has been reduced to 95% of measured electrical power (DC-KW) to account for the heat dissipation along the electrical cables to the FPS.

Pressure difference along the Riser is depicted in Figure 34, where experimental and RELAP5 results are compared. Good agreement is found during the assisted circulation phase, while a slight overestimation of simulated results are observed in natural circulation phase.

Riser pressure difference is employed to obtain, by an indirect derivation, the experimental value of the mean argon void fraction along the Riser. The latter value is adequately predicted by RELAP5 simulated results, as shown in Figure 35.

The available driving force, during the assisted circulation phase, has been evaluated from RELAP5 results as follows:

$$\Delta P_{DF} = \Delta\rho \cdot g \cdot H_r \qquad (9)$$

where H_r is the Riser height, set to 3.7 m, g the gravity acceleration and $\Delta\rho$ is defined as:

$$\Delta\rho = \bar{\rho}_{LBE} - \rho_{r,TP} \qquad (10)$$

where $\bar{\rho}_{LBE}$ and $\rho_{r,TP}$ are respectively the LBE mean density and the two phase flow mean density inside the Riser; these values are directly supplied by the code. The driving force obtained by the code is plotted in Figure 36 and gives a value around 325 mbar.

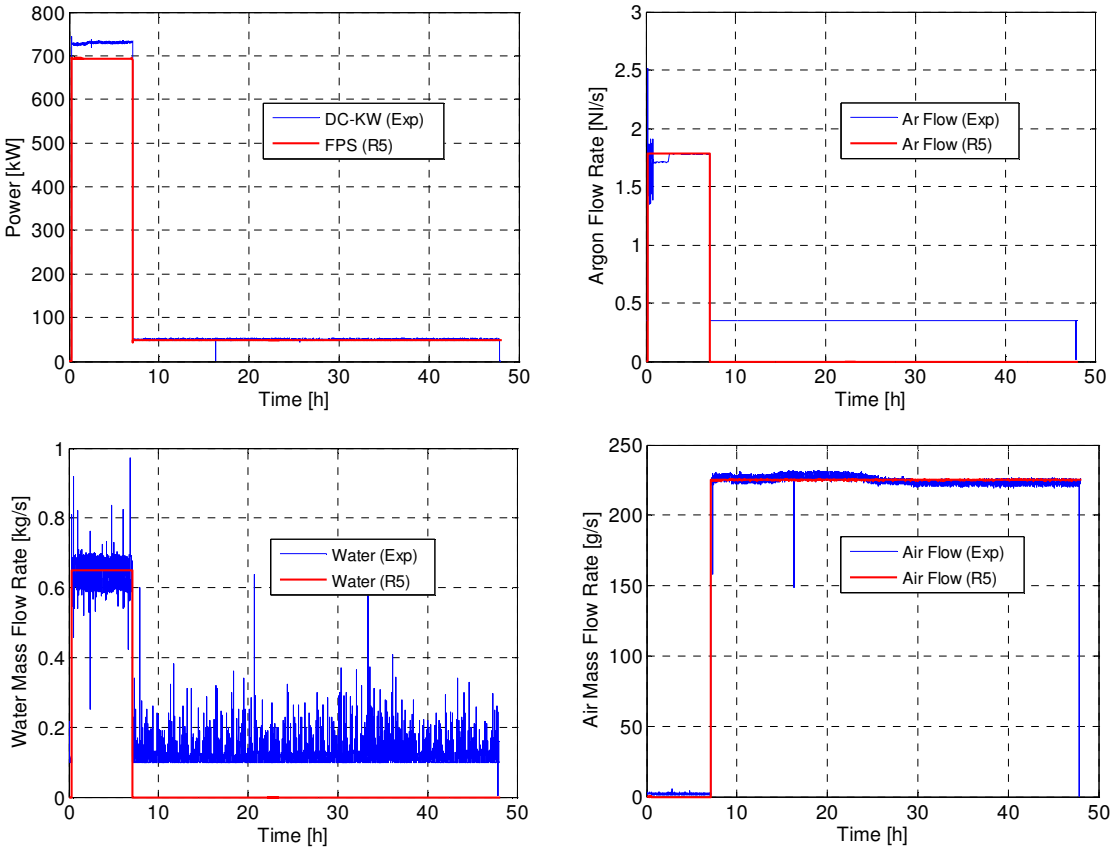

Figure 33: Test boundary conditions (FPS Power, Argon Flow Rate, HX Feed Water, DHR Air Flow Rate)

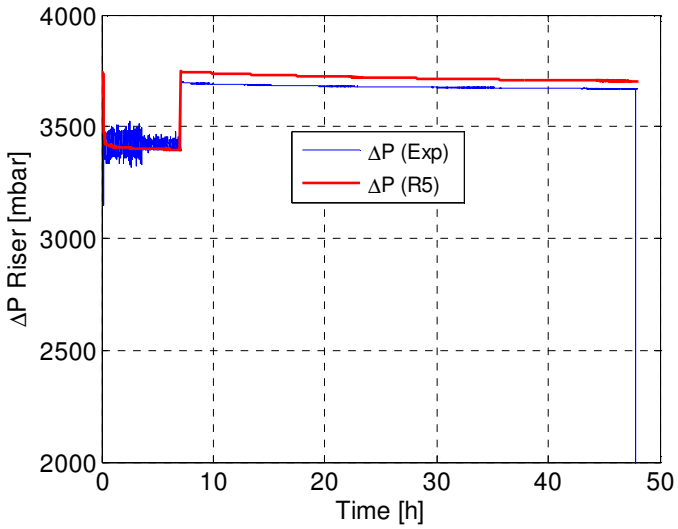

Figure 34: Pressure difference in the Riser

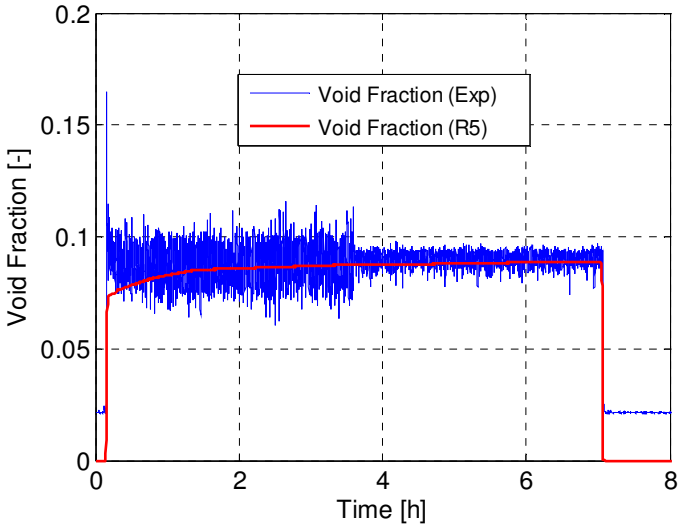

Figure 35: Average void fraction into the Riser

Measured and simulated values of LBE mass flow rate along CIRCE main flow path are compared in Figure 37, showing a good agreement both in forced and natural circulation regimes.

The value of the mass flow rate through DHR predicted by the code is reported as well.

During assisted circulation (first 7 h) LBE mass flow rate, measured in the FPS, is characterized by wide oscillation with an average value of 56.5 kg/s which is adequately reproduced by the code.

As soon as PLOH+LOF transient initiates, at about 7 h, stable natural circulation in the primary circuit is established; measured and simulated values are about 7.2 kg/s and 7.7 kg/s respectively.

The predicted DHR mass flow rate shows a progressive increase, and stabilizes at 6.9 kg/s at about 9 h.

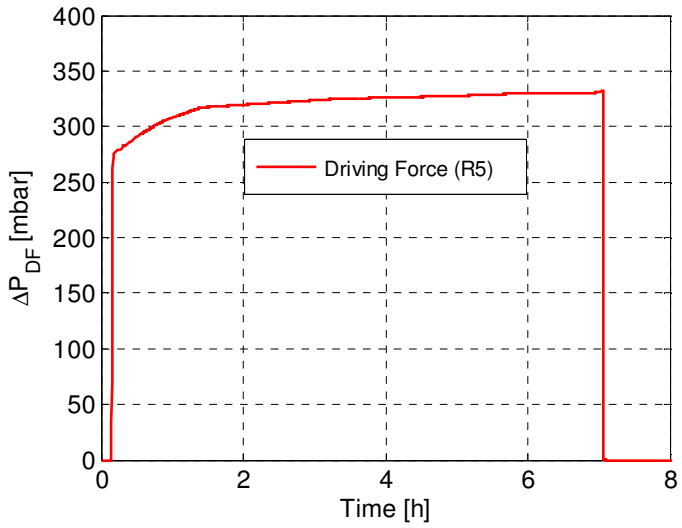

Figure 36: Driving Force available for LBE circulation

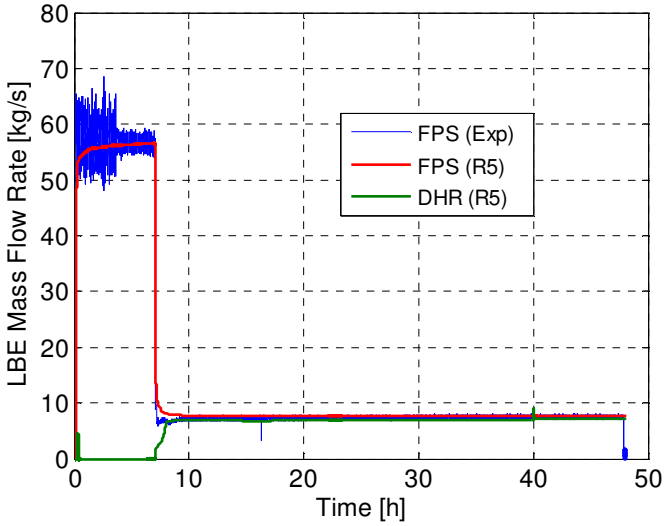

Figure 37: FPS and DHR mass flow rate

Experimental inlet and outlet FPS temperature evolution during the test are shown in Figure 38 and compared with RELAP5 results. The code satisfactorily simulates the temperature trend related to the full power assisted circulation phase during the first 7 h, reaching a stationary values of about 370°C and 284°C for FPS outlet and inlet temperatures respectively.

The onset of natural circulation and power reduction (about 7 % of nominal power) following the PLOH+LOF event, produces a sudden drop of the previous FPS temperatures to 322°C and 280°C.

From those values, temperatures increase till the end of the test (t=48 h) without reaching a stationary condition.

The trend obtained by the code during this transient is similar to the experimental one, however it presents some discrepancies probably ascribed to some uncertainties in defining the DHR system efficiency as well as the evaluation of the facility heat losses towards the environment.

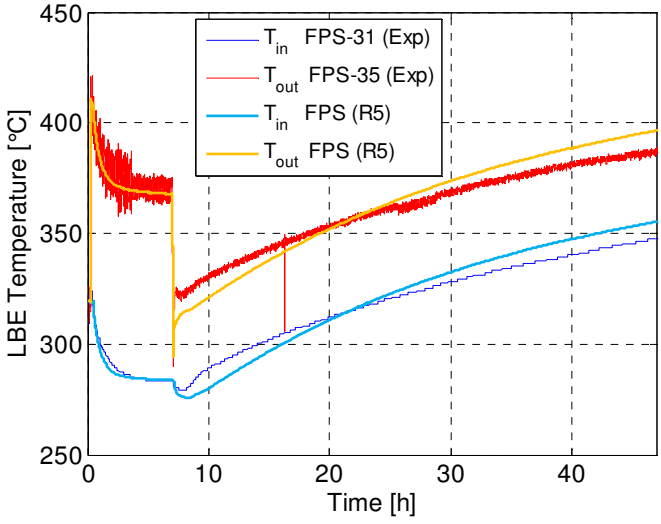

Figure 38: FPS inlet and outlet temperatures

6. CONCLUSIONS

The experiment performed on the CIRCE pool facility consisted of a full power steady state run followed by a protected loss of flow and cold sink (PLOF+PLOH). For the run of the experiment the FPS, representative of LFR fuel assembly, has been deeply instrumented aiming to investigate the thermal-hydraulic behaviour of a fuel bundle cooled by LBE, both under forced and natural circulation. The available instrumentation allowed to evaluate the Nusselt number (and thus the HTC) of the fuel pin bundle, under the transient scenario simulated.

As results, the Nusselt number along the FPS is constant and close around 22 under forced circulation (LBE velocity ~ 1m/s) and full power (q" ~ 80 W/cm^2), and it falls down close around 13 under natural circulation (LBE velocity ~ 0.15 m/s) and decay power (q" ~ 5 W/cm^2). Thus, the results carried out have shown as the primary system of LFR nuclear system is technological feasible.

Further experimental tests are needed in order to better understand the involved phenomena and to investigate the pool behavior and concerning the thermal power removed by the HX at full power steady state condition and the LBE mass flow rate in the DHR-system after its activation. In addition, thermal stratification inside the LBE pool needs to be deeply investigated in further tests, especially under natural circulation condition.

Anyway the experimental data already collected during the ICE activity will allow to improve and validate physical model (turbulence model for CFD tools) as well as numerical tools (system codes) when employed on HLM pool system.

In particular the performed post-test analysis demonstrates the suitability of RELAP5 model to simulate CIRCE-DHR experiment representative of a PLOH+LOF transient. LBE primary flow is adequately reproduced by the code in both assisted and natural circulation conditions, including the transition from one regime to the other.

Likewise the values of the pressure difference and gas void fraction inside the Riser are well predicted. The model properly simulates HX power removal and attainment of stabilized condition during the full power run, whereas some discrepancies remain in the simulation of the transient conditions characterized by reduced power supply and the activation of the DHR system, probably due to the uncertainty in the DHR modeling and the quantification of the facility heat losses.

7. REFERENCES

[1] P. Turroni, L. Cinotti, G. Corsini, L. Mansani, "The CIRCE Facility", AccApp'01&ADTTA'01, Nuclear Application in the new Millennium, Reno (Nevada-USA), November 11-15, 2001.

[2] G. Benamati, G. Bertacci, N. Elmi, G. Scaddozzo, "Report on Gas Enhanced Circulation Experiments and Final Analysis (TECLA D41)", Report ENEA HS-A-R-016, 2005.

[3] G. Bandini, I. Di Piazza, P. Gaggini, A. Del Nevo, M. Tarantino, "CIRCE experimental set-up design and test matrix definition", ENEA UTIS-TIC Technical Report, IT-F-S-001, 28/02/2011.

[4] M. Tarantino, G. Scaddozzo, "Test specifications of the Integral Circulation Experiments", Report ENEA ET-F-S-001, Deliverable D. 4.15, DM4 DEMETRA, IP-EUROTRANS, 2006.

[5] A. Barbensi, G. Corsini, "Specification for the EFIT primary system", Deliverable D. 1.4, DM1 DESIGN, IP-EUROTRANS, 2006.

[6] B. Giraud, "Review and justification of the main design options of XT-ADS", Deliverable D. 1.5, DM1 DESIGN, IP-EUROTRANS, 2006.

[7] C. Artioli,"Specification for the EFIT Core and Fuel Element Design", Deliverable D. 1.6, DM1 DESIGN, IP-EUROTRANS, 2006.

[8] G. Van den Eynde,"Specification for the XT-ADS Core and Fuel Element Design", Deliverable D. 1.7, DM1 DESIGN, IP-EUROTRANS, 2007.

[9] L. Mansani, "Candidates Materials for XT-ADS and EFIT, Operating Conditions and Testing Requirements", Deliverable D. 4.1, DM4 DEMETRA, IP-EUROTRANS, 2005.

[10] W. Ambrosini, M. Azzati, G. Benamati, G. Bertacci, L. Cinotti, N. Forgione, F. Oriolo, G. Scadozzo, M. Tarantino, "Testing and qualification of CIRCE instrumentation based on bubble tubes", Journal of Nuclear Materials, pp. 293-298, 2004.

[11] G. Benamati, C. Foletti, N. Forgione, F. Oriolo, G. Scaddozzo, M. Tarantino, "Experimental study on gas-injection enhanced circulation performed with the CIRCE facility", Nuclear Engineering and Design, vol. 237, pp. 768-777, Iss. 7, 2007.

[12] N. Todreas, M. Kazimi, "Nuclear System I - Thermal Hydraulic Fundamentals", Tylor&Francis, 1993.

[13] V.I. Subbotin, P.A. Ushakov, P.L. Kirillov, M.H. Ibragimov, M.N. Ivanovski, E.M. Nomofilov, D.M. Ovechkin, L.N. Sorokin, V.P. Sorokin, "Heat transfer in elements of reactors with a liquid metal coolant", In: Proceedings of the 3rd International Conference on Peaceful Use of Nuclear Energy, 8, NY, pp. 192–200, 1965.

[14] K. Mikityuk, "Heat transfer to liquid metal: review of data and correlations for tube bundles", Nuclear Engineering and Design, Vol. 239, 680–687, 2009.

[15] P.A. Ushakov, A.V. Zhukov, M.M. Matyukhin, "Heat transfer to liquid metals in regular arrays of fuel elements, High Temperature, Vol. 15, pp. 868–873, 1977; translated from Teplofizika Vysokikh Temperatur 15 (5), pp. 1027–1033, 1977.

[16] V.H. Gräber, M. Rieger, "Experimentelle Untersuchung des Wärmeübergangs an Flüssigmetalle (NaK) in parallel durchströmten Rohrbündeln bei konstanter und exponentieller Wärmeflussdichteverteilung", Atomkernenergie (ATKE) Bd. 19, 23–40, 1972.

[17] RELAP5/MOD3.3 Code Manual, "NUREG/CR-5535-Vol.I-VIII", January 2002.

8. Abbreviations and acronyms

CIRCE	CIRcolazione Eutettico
DAQ	Data AQuisition system
DHR	Decay Heat Removal
ENEA	Agenzia nazionale per le nuove tecnologie, l'energia e lo sviluppo economico sostenibile
EFIT	European Facility for Industrial Transmutation
FPS	Fuel Pin Simulator
HLM	Heavy Liquid-Metal
HS	Heat Source
HX	Heat Exchanger
HTC	Heat Transfer Coefficient
ICE	Integral Circulation Experiments
LabVIEW®	Laboratory Virtual Instrument Engineering Workbench
LBE	Lead-Bismuth Eutectic
LOF	Loss of Flow
LOFA	Loss Of Flow Accident
LMFR	Liquid Metal Fast Reactor
Nu	Nusselt number
Pe	Peclet number
PLOHS	Protected Loss Of Heat Sink
TC	Thermocouple
THINS	Thermal Hydraulic of Innovative Nuclear System
XT-ADS	Experimental Accelerator Driven System